Activation-induced shift in nutrient preference and function-specific nutrient dependence in human neutrophils

Emily C. Britt (1,2), Xin Qing (1,2), James A. Votava (1), Jorgo Lika (1,3,4), Andrew Wagner (5), Simone Shen (5), Nicholas L. Arp (1,3,4), Hamidullah Khan (6), Stefan M. Schieke (6), Christopher D. Fletcher (7), Anna Huttenlocher (3,4,5,8,9) Jing Fan (1,2,3,4,10)

1 Morgridge Institute for Research, Madison, WI, USA.
2 Department of Nutritional Sciences, University of Wisconsin-Madison, Madison, WI, USA.
3 Cell and Molecular Biology Graduate Program, University of Wisconsin-Madison, Madison, WI, USA.
4 University of Wisconsin Medical Scientist Training Program, University of Wisconsin School of Medicine and Public Health, Madison, WI 53792
5 Department of Medical Microbiology and Immunology, University of Wisconsin-Madison, Madison, WI, USA.
6 Department of Dermatology, University of Wisconsin-Madison, Madison, WI, USA.
Department of Dermatology, Georgetown University Medical Center and Washington DC VA Medical Center, Washington, D.C., USA
7 University of Wisconsin Carbone Cancer Center, Madison, WI, USA
8 Comparative Biomedical Sciences Graduate Program, University of Wisconsin-Madison, Madison, WI, USA
9 Department of Pediatrics, University of Wisconsin-Madison, Madison, WI, USA.
10 jfan@morgridge.org

Abstract

Neutrophils are the first responders in innate immunity. Neutrophils can perform a variety of effector functions which are associated with specific metabolic demand. The utilization of various metabolic sources, including extracellular glucose, intracellular glycogen, and other alternative substrates, have been found critical for neutrophil fitness and functions in recent studies. However, the quantitative contribution of these nutrients under specific conditions and the relative dependence of various cell functions on specific nutrients remain unclear. Here using *ex vivo* and *in vivo* isotopic tracing, we revealed that under resting condition, human peripheral blood neutrophils, in contrast to *in vitro* cultured human neutrophil-like cell lines, rely on glycogen as a major direct source of glycolysis and pentose phosphate pathway. Extracellular glucose contributes slightly less than half, and other sources have minor contributions. Upon activation with a diversity of stimuli (including zymosan A, TNFα, PMA, LPS, or *Pseudomonas aeruginosa*), neutrophils undergo a significant nutrient preference shift, with glucose becoming the dominant metabolic source. The shift to glucose utilization is often rapid and driven by multi-fold increases in glucose uptake, which is mechanistically mediated by the phosphorylation and translocation of GLUT1. At the same time, cycling between gross glycogenesis and glycogenolysis is also substantially increased, while the net flux favors sustained or increased glycogen storage. Different effector functions of activated neutrophils have specific nutrient dependence. The oxidative burst is most dependent on extracellular glucose, while the release of neutrophil extracellular traps can be flexibly supported by either glucose or glycogen utilization. Shifting neutrophil away from glycogen utilization increases migration and fungal control. Together, these results quantitatively characterize fundamental features of neutrophil metabolism and elucidate how metabolic remodeling supports and shapes neutrophil functions upon activation.

Introduction

Neutrophils are the most abundant circulating leukocytes that provide the first line of defense. Neutrophils are charged with metabolically demanding immune functions such as oxidative burst, phagocytosis, and neutrophil extracellular trap (NET) release[1,2]. To support the high and dynamically changing metabolic demands, glycolysis has long been the accepted as the main source of energy for mature neutrophils[3]. Despite the presence of mitochondria with complex networks[4], inhibition of oxidative phosphorylation does not significantly impact ATP production[5,6]. Pentose phosphate pathway (PPP) has also been found critical for some immune functions in neutrophils, particularly oxidative burst[7–10]. These crucial metabolic pathways can be supplied by different nutrient sources, including exogenous glucose or intracellular glycogen storage, both of which feed into the production of glucose-6-phosphate (G6P), the common precursor for glycolysis and PPP. Prior research has suggested the importance of both glucose metabolism and glycogenolysis in immunity. For instance, increased glucose uptake by GLUT1 is essential for CD4 T cell activation and function[11], while glycogenolysis is essential for fueling CD8 memory T-cells recall and the early response of dendritic cell activation[12,13]. Particularly in neutrophils, uptake of extracellular glucose has been reported to increase when neutrophils are exposed to classical activators or pathogens (including *Francisella tularensis, leishmania, Candida albicans*) [14–20]. On the other hand, neutrophils also possess meaningful glycogen storage, and glycogenolysis is increased by some stimulations or diseases[3,6] . Moreover, despite neutrophils relatively few mitochondria and low mitochondrial energy generation, it has been reported that mitochondrial substrates can support prolonged oxidative burst[21] and the release of NETs[22], and that neutrophils express key gluconeogenic enzymes including mitochondrial PEPCK, therefore, have the potential to generate glycolytic intermediates or glycogen store from gluconeogenic substrates. Although these recent studies clearly suggested that neutrophils have the capacity to utilize a range of nutrients to support their metabolism, survival and function, and neutrophil activation is associated with significantly reprogramming of nutrient metabolism, the quantitative contributions of these nutrients under specific conditions remained unclear.

Here we specifically quantified the contributions of major metabolic sources in neutrophils in the resting state as well as upon activation by a variety of stimuli. Furthermore, in light of accumulating evidence suggesting that physiological environment and specific cell intrinsic factors can significantly alter metabolism and cause metabolic diversity, we quantitatively evaluated the nutrient preference of human neutrophils *in vivo* by isotopic tracing in healthy volunteers, as well as *ex vivo* (freshly insolated human peripheral blood neutrophils immediately assessed in culture condition) and *in vitro* (in widely used stable neutrophil-like cell line cultured in media). This study reveals fundamental features of human neutrophil metabolism and elucidates the specific metabolic rewiring induced by different stimulations and conditions.

Beyond nutrient preference, another important metabolic question in immune responses is nutrient dependence. Neutrophils are the first innate immune cells to be recruited to sites of infection and injury, thus they can encounter changing microenvironments with varied nutrient levels. Some metabolic sources, though preferred under optimal conditions, may be compensated for by other options when unavailable, while others may be indispensable for certain effector functions. To what extent neutrophils have the flexibility to use different metabolic sources to support the initiation and maintenance of their functions has important implications in health and disease. Here we quantitatively assessed the reliance of an array of neutrophil phenotypes and functions on the two major nutrient sources, glycogen and glucose, and found that the nutrient dependence is highly function-specific. Given that dysregulation of neutrophil functions contributes to many infectious diseases and inflammatory conditions, understanding such significant and function-specific responses to metabolic perturbation can suggest corresponding therapeutic applications.

Results

Primary human neutrophils use glycogen storage as a major metabolic source in the resting state

Recent studies have revealed that the cells' nutrient utilization can be significantly impacted by nutrient availability and extracellular signals in their environment[23,24]. To characterize the nutrient preference of human neutrophils in their physiological environment, we applied an in-human isotopic tracing approach. Healthy volunteers were intravenously infused with uniformly labeled glucose tracer (U-^{13}C glucose in sterile saline, infused with an initial bolus of 8g in 10min., followed by a steady infusion rate of 8g/ h, following previously developed methods[25–27]), and blood samples were collected at various time points for analysis of metabolites in plasma and in peripheral blood neutrophils (Fig. 1a).

Plasma glucose labeling quickly enriched to ~40% labeled within 10 min and stayed mostly steady up to 60 min. (Fig.1b), while total glucose level maintained in a normal range (Supp. Fig. 1a). During this time, the majority of labeled glucose remains uniformly labeled, with a small fraction (<5%) of other label forms (M+1 to M+5) slowly arising over time, indicating metabolic turnover of glucose by tissues via gluconeogenesis. Plasma lactate, which has been recently identified as a major glucose-derived circulating metabolite[28,29] gradually increased to ~15% labeled (Supp. Fig. 1b). Other circulating metabolites, including glycerol, which may directly contribute to lower glycolysis, glutamine, glutamate, and alanine remain minimally labeled in plasma (Supp. Fig. 1c-f). These are the major circulating metabolites available to neutrophils that can potentially deliver labeling in cells.

In neutrophils, intracellular glycolytic intermediates quickly gained labeling after infusion. The dominant labeling forms, including 3- and 6- labeled fructose-1,6-bisphosphate (FBP) and 3-labeled dihydroxyacetone phosphate (DHAP), indicate direct contribution of circulating glucose via glycolysis (Fig 1c). A smaller fraction are other label forms, including 1- or 2- labeled were observed. This may result from either scrambling non-oxidative PPP, which we found is highly reversible in resting neutrophils[7], or to a less extent, from gross flux from phosphoenolpyruvate derived from phosphoenolpyruvate carboxykinase (PEPCK). There is a small fraction of labeling in intracellular TCA cycle intermediates during this time frame (Supp. Fig. 1g). The average labeling enrichments of glycolytic intermediates stay mostly steady from 30min to 60min (Fig. 1d). This average labeling enrichment normalized to the labeling enrichment of plasma glucose is the maximal direct contribution circulating glucose may have to glycolysis[30]. This ratio stays around 50% (Fig. 1d) indicating the direct contribution of plasma glucose is around or slightly less than 50%.

We further assessed the utilization of glucose in freshly isolated primary human neutrophils cultured *ex vivo* in culture media (Fig.1a). Extracellular glucose labeled slightly less than 50% of the glycolytic intermediates across donors (Fig. 1e), with the dominant label forms reflecting the direct contribution via glycolysis (Supp. Fig. 1h), and glucose minimally labeled TCA cycle intermediates (Supp. Fig. 1i). These results showed the utilization of glucose is similar *ex vivo* compared to *in vivo* conditions, contributing to slightly less than 50% of glycolysis, and there were other important nutrients acting as the direct source supplying the metabolism of primary human neutrophils under the resting condition.

To understand the other major direct metabolic sources, we tested the contribution of intracellular glycogen, which was suggested by recent studies as important for supplying glycolysis across multiple tissues and for neutrophil survival and functions[6,18,30]. Inhibiting utilization of glycogen by

the treatment of glycogen phosphorylase inhibitor (GPi) brought the glycolytic intermediates labeling from extracellular glucose to near complete (Fig. 1e, Supp. Fig. 1h). We estimated the contribution of glycogen by quantifying the increase in labeling enrichment when glycogenolysis is blocked (+GPi) compared to baseline (-GPi), and found it is ~50% for glycolysis intermediates (Fig. 1f). While glucose and glycogen combined can account for the majority of direct nutrient sources, other sources may have a minor contribution (<10%). For instance, we observed significantly less labeled glycerol-3-phosphate (G3P) relative to DHAP both with or without GPi (Supp. Fig. 1j). The additional unlabeled G3P can be generated from unlabeled sources, such as lipid degradation, which can further incorporate into lower glycolysis.

Unlike primary human neutrophils assessed *in vivo* or *ex vivo*, which both showed a ~50:50 mixed nutrient preference towards glucose and glycogen, we found human neutrophil-like cell line HL-60 cultured *in vitro* were primarily dependent on extracellular glucose as the direct source for glycolytic intermediates. Extracellular glucose labeled nearly all of the glycolytic intermediates and treatment of GPi had minimal effect (Fig.1g). This is consistent with recent reports in T-cells[31] that freshly isolated cells *ex vivo*, but not *in vitro* cell models, reflect *in vivo* metabolic phenotype faithfully, likely because significant metabolic changes accumulate during prolonged *in vitro* culturing.

Stimulation induces nutrient preference shift toward primarily using extracellular glucose

As results above revealed both extracellular glucose and intracellular glycogen are major nutrients for primary human neutrophils at resting state, we next investigated whether such nutrient preferences change when neutrophils are activated by a variety of stimulation signals. Primarily human peripheral blood neutrophils were stimulated *ex vivo* with phorbol myristate acetate (PMA), zymosan A (Zym), TNFα, or heat inactivated *Pseudomonas aeruginosa* (HI PsA, heat inactivation prevents the interference of bacterial metabolism) for 30 minutes, or LPS for 4 hours, and we traced the incorporation of extracellular U-^{13}C-glucose into glycolytic intermediates as an indication of glucose utilization. There was a significant increase in the labeling of all glycolytic intermediates to 80-90% upon activation with each of these stimuli (Fig. 2a). Similarly, intermediates of the pentose phosphate pathway also showed significantly increased labeling from extracellular glucose upon activation (Fig. 2b). These data indicate a substantial nutrient preference shift with extracellular glucose becoming the dominant direct source for glycolysis and pentose phosphate pathway in activated neutrophils.

Mirroring this, the contribution of glycogen to glycolysis, as measured by the gain of labeling from glucose when cells were treated with GPi, reduced substantially (Fig. 2c). The contribution by other sources beyond glucose and glycogen, as indicated by the fraction of glycolytic intermediates remaining unlabeled from glucose after glycogen degradation was inhibited, remained less than 10% in activated neutrophils (Fig. 2d).

While all the investigated stimuli induce similar nutrient preference shift, it occurs with different kinetics. Zymosan induced a very rapid shift, with glucose becoming the dominant source within 15min after stimulation (Fig. 2e). In contrast, LPS induced a much slower shift over 2 hours (Fig. 2f).

The shift to glucose utilization is driven by a substantial increases in glucose uptake by GLUT1

The stimulation induced nutrient preference shift could be driven by increase in glucose utilization or decreased glycogen utilization (Fig.3a). Therefore, we first measured glucose consumption rate. A 4-6 fold increase in total glucose consumption was observed within 1 hour after stimulation with zymosan, TNFα, and PMA (Fig. 3b). The level of GLUT1, one of the main glucose

transporters in neutrophils[20,32], on the cell surface increased as soon as 30 minutes after stimulation (Fig. 3c), which would enable the rapid increase in glucose uptake. It was reported that GLUT1 can be phosphorylated by PKC, and the phosphorylation enhances its localization to the cell surface[33], . Moreover, both zymosan and TNF can activate PKC[34,35], and PMA is a direct activator of PKC, pointing to likely mechanisms for increased GLUT1 on plasma membrane within 30min. Indeed, we found while total cellular level of GLUT1 remains mostly constant during this time, GLUT1 phosphorylation was increased significantly in all three conditions (Fig. 3d).

Glycogen degradation is regulated largely by the phosphorylation of glycogen phosphorylase (PYGL) (Fig. 3a). Therefore, we probed the level and phosphorylation of PYGL. In cells stimulated with PMA, zymosan, and TNFα, there was no significant change in total PYGL level, however, phosphorylation of PYGL (Ser15) was increased (Fig. 3e). Phosphorylated PYGL is the active form. This data suggests the gross flux of glycogenolysis is likely still increased upon stimulation, despite the relative preference shifts toward less glycogen contribution, because the profound increase of glucose uptake can dominate the relative contribution from glycogen.

Glycogen cycling is increased upon neutrophil activation

Although PYGL is increasingly phosphorylated upon neutrophil activation, indicating increased glycogen degradation activity, the total glycogen storage level in cells trends towards slight increase upon stimulation of zymosan or LPS (Fig 3f), suggesting further increased gross glycogen synthesis flux that result in net balance or accumulation of intracellular glycogen. We measured the labeling of intracellular glycogen after cells are cultured in media containing U-^{13}C-glucose for 2h, which indicates glycogen turnover during this period. The glycogen labeling increased from <2% within 2h in resting state to ~10% in zymosan or LPS stimulated neutrophils (Fig. 4g), and the extent of glycogen labeling increase exceeds the increase of labeling of UDP-glucose (Supp. Fig. 2a), the precursor of glycogen synthesis. These results suggest that upon neutrophil activation, glycogen cycling, including both gross glycogen synthesis and glycogen degradation, is activated, and the net flux favors glycogen synthesis to cause increased glycogen storage, which may help prepare cells for being recruited to low glucose microenvironment.

Increased glucose utilization supplies essential metabolic reactions in activated neutrophils

Increased glucose uptake, as well as increased PYGL activity, would increase the production rate of G6P, a common upstream metabolite supplying important biosynthetic and energy producing pathways. The production of lactate increased substantially over 1h after stimulation with zymosan, TNFα, or PMA (Fig. 4a), indicating increased glycolysis rate. We previously showed that oxidative PPP flux is greatly upregulated in activated neutrophils to enable oxidative burst[7]. Indeed, upon stimulation of PMA, zymosan, TNFα, or HI PSA, PPP intermediates significantly accumulated by 30min, in contrast, LPS stimulation did not induce such change by 4 hour (Fig. 4b). Withdrawing extracellular glucose significantly reduced the accumulation of pentose phosphate upon stimulation. In contrast, inhibiting glycogen degradation only had a minor impact on the accumulation of PPP intermediates, and combination of glucose withdrawal and glycogen utilization inhibition has the strongest effect (Fig. 4c). This result, consistent with the glucose labeling showing extracellular glucose became the dominant source of PPP upon activation (Fig. 2b), suggests increased glucose utilization is essential to support the upregulation of PPP.

In neutrophils under resting condition, we observed the incorporation of labeled glucose into TCA cycle occurs slowly and to a minor level, with most TCA cycle intermediates only labeled ~5% by 6 hours (Fig. 4d). The low baseline activity of TCA cycle is consistent with previous literature

suggesting that neutrophils have few classic mitochondria[4,5]. Upon activation with zymosan, we found a rapid and substantial increase in TCA cycle labeling, with citrate labeling up to 20% within 1 hour (Fig. 4d), which exceeds the extent of increased glycolytic intermediates labeling from glucose. This result suggests that upon activation, increased flux was sent through TCA cycle, supported by increased glucose utilization. Nonetheless, the overall fraction of TCA cycle labeling is relatively small (<20%) within the short period after stimulation, suggesting TCA cycle turnover is a relatively slow process for glucose utilization, and there may be other important sources for TCA cycle in neutrophils. Consistently, glucose withdrawal or glycogenolysis inhibition within a short period does not significantly reduce the level of TCA cycle intermediates (Supp. Fig. 2b).

When neutrophils are stimulated, a series of immune functions are activated, which are associated with substantial metabolic demands. Nonetheless, the cellular energy status is generally well-maintained upon stimulation (Fig. 4e), suggesting the increased glucose utilization (and gross glycogen utilization) is sufficient to support the increased bioenergetic demand upon activation. We found that inhibiting glycogen utilization or withdrawing extracellular glucose alone did not substantially reduce energy charge in stimulated neutrophils. While inhibiting both more noticeably reduced energy charge (Fig. 4e, Supp. Fig. 2c). This suggests neutrophils are able to use either glycogen or glucose to maintain energy status, which can provide basis for their metabolic flexibility to support cell functions under different nutrient conditions.

Extracellular glucose greatly impacts oxidative burst and late-time cell death

The reprogramming of cellular metabolism plays a key role in supporting immune functions neutrophils perform quickly upon activation. We next examined the dependence of these functions on the two major metabolic sources identified, glucose and glycogen, by acutely limiting the utilization of either one or both. Blocking glycogenolysis with glycogen phosphorylation inhibitor, glucose withdrawal, or the combination of both, did not largely reduce cell viability within the short period (Supp. Fig. 3a). A day after primary neutrophil isolation, a large portion of the cells died, which is consistent with neutrophils' short-lived nature (Supp. Fig. 3b). Interestingly, although the overall survival rates at this time point are similar (Supp. Fig. 3b), in conditions where neutrophil are cultured with extracellular glucose, a large portion of neutrophils die through apoptosis, while in conditions without glucose, cell death is primarily observed through non-apoptotic mechanism, demonstrating that nutrient condition can significantly affect cell death (Fig. 5a). Nonetheless, for assaying cell functions, we focused on the first few hours after neutrophil isolation as neutrophils are first responder in innate immunity and perform their functions rapidly. During this period, cells remained highly viable across all nutrient conditions (Supp. Fig. 3a).

Oxidative burst is the production of reactive oxygen species for pathogen killing, which can be induced by PMA or zymosan. Inhibiting glycogen utilization had minimal impact on oxidative burst induced by PMA or zymosan, while inhibiting extracellular glucose utilization by inhibiting hexokinase (using 2DG) or glucose withdrawal greatly reduced the oxidative burst (Fig. 5b-d). Limiting glucose utilization not only greatly reduced the overall intensity of burst (Fig. 5c), but also made the oxidative burst start to decline faster, particularly noticeable with lower dose stimulation, which induces a slower burst (Fig. 5d). This is consistent with neutrophils relying heavily on glycogen utilization at baseline, but switching to primarily using glucose soon after stimulation, thus when extracellular glucose is absent, oxidative burst is still able to start, but soon becomes limited. The effect of inhibiting glucose and glycogen utilization appears to be additive, in the condition with no glucose and with GPi treatment, cells have the lowest amount of burst (Fig. 5b). Together, these results showed the oxidative burst in stimulated neutrophils was supported primarily by glucose, with glycogen providing a very minor contribution.

Neutrophil extracellular trap release and phagocytosis can be flexibly supported by either glucose or glycogen

Contrasting with oxidative burst, inhibiting the utilization of either extracellular glucose or intracellular glycogen utilization only decreased NET release slightly, however, inhibiting both completely abolished NET release. This suggests neutrophils have great flexibility to use either nutrient source to support NETosis, but at least one of these sources is required and cannot be compensated by other alternative sources (Fig. 5e).

Similar to NET release, phagocytosis of bacteria also showed flexibility. Cell can still perform phagocytosis for the most part when either glucose or glycogen utilization, or both, is limited, although the phagocytosis rate is slightly reduced when either nutrient supply is limited (Fig. 5f). For both NET release and phagocytosis, the dependence on extracellular glucose is slightly higher than glycogen.

Inhibiting glycogen utilization increases neutrophil migration and fungal control

Upon sensing signals associated with infection or inflammation, neutrophils can quickly migrate towards the site. We found neutrophil migration towards chemoattractant C5a strongly depends on glucose, as withdrawing extracellular glucose greatly inhibits migration. Conversely, inhibiting glycogen degradation with GPi, which would force cells to primarily rely on extracellular glucose (Fig. 1e), significantly increased neutrophil migration (Fig. 6a). Interestingly, when glycogen degradation inhibition is combined with glucose withdrawal, we observed an even greater suppression of neutrophil migration than glucose withdrawal alone (Fig. 6a). It is possible that the metabolic shift towards glucose utilization by GPi treatment can promote migration, however, inhibiting glycogen utilization in the condition where extracellular glucose is unavailable can significantly decrease cellular energy charge, restricting cells' ability to migrate, while inhibiting glycogen utilization alone does not (Fig. 4e).

Given the intriguing observation that glycogenolysis inhibition promotes neutrophil migration, we further assessed it in the setting of fungal infection with Aspergillus fumigatus[36]. To avoid the direct impact of GPi treatment on *A. fumigatus*, we pre-treated primary human neutrophils with GPi for 1 hour, then removed the GPi and co-incubated neutrophils with fungal germlings in fresh culture media. The inhibitory effect of neutrophil glycogenolysis by GPi is sustained up to 4hr after pre-treatment (Supp Fig. 4a). Consistently, the effect of GPi treatment on inhibiting neutrophil migration towards C5a is also sustained after acute pre-treatment (Supp. Fig. 4b). When co-cultured with *A. fumigatus*, neutrophils swarm towards, and cluster around, fungal pathogens (Fig. 6b). The percentage of neutrophil clusters around fungal hyphae is significantly increased when neutrophils were pre-treated with GPi, suggesting increased neutrophil migration towards fungal pathogens upon glycogenolysis inhibition (Fig 6c).

Neutrophils play a significant role in controlling the growth of the invasive pathogen *A. fumigatus*. Coordinated swarming towards the pathogen is associated with effective fungal control. Consistent with our finding that inhibiting glycogenolysis increased neutrophil clustering around developing *A. fumigatus* hyphae and germlings (Fig. 6b,c), the fraction of *A. fumigatus* cells that remained after 4h co-incubation with neutrophils is significantly reduced when the neutrophils were pre-treated with GPi (Fig. 6d). This result suggested shifting neutrophil away from glycogen utilization promotes fungal control.

Discussion

This work quantitatively evaluated the contributions of different nutrients in neutrophil metabolism under resting and activated states. Glycogen was found to be a major metabolic source, particularly at resting state. Neutrophils can actively turnover glycogen, and we observed such turnover is upregulated upon cell activation. The synthesis of glycogen uses UDP-glucose as the direct substrate, which is synthesized from G6P. In light of recent work which found that neutrophils express key gluconeogenic enzymes[6], the possible role of gluconeogenesis to supply glycogen storage has been brought up. We found that at gross flux level, there is a small fraction of glycolytic intermediates that does not directly arise from glucose or glycogen, which may result from gross flux at the direction of gluconeogenesis. However, such contribution is very small. At the net flux level, supplying glycogen with gluconeogenesis requires ATP production from non-glycolytic pathways to support bioenergetics. Our observation is that consistent with previous reports, TCA cycle activity in resting neutrophils is very low to produce energy. Therefore, overall, glucose is the ultimate source for neutrophil metabolism and energy supply, however, at gross flux level, a large fraction of the glucose is converted to glycogen first, and glycogen act as a major direct source for neutrophil metabolism at resting state.

A question is why primary neutrophils keep this active cycling between glucose and glycogen, rather than directly using extracellular glucose like some other cells, or even neutrophil-like cell lines. Cycling glucose with glycogen storage can provide a buffer of fluctuating glucose level. Primary neutrophils need to be actively recruited from the circulation to the site of infection, where they perform important functions. Such sites often have low microenvironmental glucose [37], therefore the ability to use glycogen storage can provide neutrophils extra metabolic flexibility, even though extracellular glucose is the preferred source for activated neutrophil when available. On the other hand, high glucose level in diabetes appears to be closely associated with multiple hyper-active phenotypes in neutrophils and altered wound healing [38–40], and hyperglycemia is detrimental during sepsis, which mirror our observation that shifting towards glucose utilization is associated with activation of certain neutrophil functions. Largely relying on glycogen utilization at the resting state rather than directly using extracellular glucose may provide more buffer against inappropriate neutrophil hyper-activation. Clinical evidence is consistent with the ability to cycle between glucose and glycogen is critical for neutrophils. Low neutrophil numbers and functional defects in neutrophils are among the most important symptoms of some subtypes of glycogen storage disease (GSD), particularly, GSD-Ib[41–44]. Interestingly, some other form of glycogen storage disease, such as GSD-Ia, has no clinical reports of similar neutrophil dysfunction[45]. GSD-1b is characterized by a deficiency in G6P transport through the ER membrane. This suggests that not only general glycogen cycling is important for neutrophils, but there may also be subcellular compartment-specific metabolism that allow neutrophils to channel glucose or glycogen utilization differently, which is critical to neutrophil function. The compartment specific role may also contribute to some of the function-specific dependence on glucose or glycogen we reported here.

Our results here revealed that different neutrophil functions have different flexibility to use glucose or glycogen to compensate for each other. These functions have diverse metabolic demands. The specific type of their major metabolic demand and the size and kinetic requirement of such metabolic demand are likely to contribute to the function-specific nutrient dependence. Oxidative burst requires neutrophils to generate a large amount of NADPH in a short period of time to fuel ROS production via NADPH oxidase. We had previously shown that the rapid NADPH production is dependent on substantial upregulation of PPP[7]. Here we found the PPP upregulation is primarily supported by glucose, which cannot be compensated for by glycogen (Fig. 4c). This is likely because activated neutrophils can use extracellular glucose to supply substrates at much higher gross flux than cells can utilize glycogen (as indicated by the labeling results), even though

the ability to use both nutrient sources is activated. Therefore, glucose, the fast-accessible source, has an irreplaceable role in supporting the high metabolic demands of oxidative burst, and the effects of glucose withdrawal or glycogen degradation inhibition on oxidative burst mirror their effects on PPP (Fig. 5b-d). On the other hand, other functions may primarily require energy supply, and associated with lower metabolic demands that are not as kinetically limited. For instance, NET release only needs a low level of ROS to signal for its activation[46]. We found that activated neutrophils can largely maintain their energy status with either glucose or glycogen, as long as at least one of the sources is available (Fig. 4e). Such functions with moderate demands are more likely to have high flexibility to be supported by either nutrient.

This study found that neutrophils' nutrient preference shifts significantly upon activation, and diverting neutrophils' nutrient utilization can significantly alter their functions in a function-specific way. This has several implications for health. Neutrophil functions must be properly controlled, promoting pathogen eliminating functions can be beneficial for infectious diseases, while lowering pro-inflammation response can alleviate inflammatory conditions. Metabolic manipulation is a promising avenue for shaping immune response. Elevated glucose uptake has been recognized a hallmark of activated T cells, B cells, and macrophages and therefore has been probed as a therapeutic target for various disease[47,48]. Such research in neutrophils had been significantly lagging. Here we showed that limiting glucose uptake specifically suppresses oxidative burst, which can cause tissue damage, while several other functions and overall neutrophil survival are not sensitively affected by it. We also made the intriguing finding that shifting neutrophils away from glycogen utilization promotes migration and fungal control. The exact mechanism requires further investigation; however, it is consistent with that treatment with glycogenolysis inhibitor causes a shift towards increased glucose utilization, both in relative contribution and in absolute rate, which mimics the shift induced by activation. The findings of specific metabolism-function connections point to the relevance of both altered nutrient metabolism contributing to specific diseases and targeting specific nutrient metabolism to treat disease. Future research is needed to investigate whether alteration in nutrient levels in specific biological environment impacts disease through changing neutrophil metabolism, and to further elucidate the exact molecular mechanism underlying the specific connections between nutrient metabolism and neutrophil functions.

Figure Legends

Figure 1. Contribution of glucose and glycogen in the metabolism of human neutrophils in the resting state.

a. Schematic of *in vivo* and *ex vivo* U-^{13}C-glucose tracing.

b. Plasma glucose labeling over a time course following U-^{13}C-glucose infusion. Results show mean ± SD from n=3 independent participants.

c. Full isotopic labeling distribution of intracellular fructose-1,6-bisphosphate (FBP), and dihydroxyacetone phosphate (DHAP) from neutrophils isolated from blood sample pre-infusion (0min), 30 or 60 minutes of U-^{13}C-glucose infusion for each participant.

d. Average labeling enrichment (on a per carbon basis) of intracellular glycolytic metabolites from neutrophils isolated from blood after 30 or 60 minutes of U-^{13}C-glucose infusion, normalized to the labeling enrichment of plasma glucose. Bars and error bars show mean ± SD from n=3 independent participants, represented by different markers.

e. Average labeling enrichment of glycolytic metabolites (on a per carbon basis) from peripheral blood neutrophils incubated *ex vivo* in U-^{13}C-glucose media for 30 minutes with or without treatment of 20μM glycogen phosphorylase inhibitor (GPi). Bars and error bars show mean ± SD from n=3 independent donors.

f. Difference between labeling enrichment of glycolytic intermediates from unstimulated neutrophils treated with GPi compared to untreated. Bars and error bars show mean ± SD from n=3 independent donors.

g. Full isotopic labeling distribution of intracellular glycolytic intermediates from HL-60 cells following 30-minute incubation in U-^{13}C-glucose media with or without GPi treatment. Results show the average of technical replicates from one representative experiment. Unstimulated labeling results were confirmed in 3 independent experiments.

Figure 2. Nutrient preference shift in neutrophils upon activation.

a-b. Labeling patterns of glycolytic intermediates (a) and pentose phosphate pathway intermediates (b) from U-^{13}C-glucose in human peripheral blood neutrophils that are unstimulated (n=5 donors), 30min after stimulation with 100nM PMA (n=4 donors), 300μg/mL zymosan A (n=5 donors), 100ng/mL TNFα (n=3 donors), or heat inactivated *P. aeruginosa* (HI PsA, 10:1 bacteria: neutrophil) (n=3 donors), or 4h after stimulation with 1ug/mL LPS (n= 3 donors). Bars and error bars show mean ± SD.

c. Increase in average label enrichment of indicated glycolytic intermediates from U-^{13}C-glucose caused by treatment of GPi (20μM), in neutrophils that are unstimulated or stimulated with indicated signals. Bars and error bars show mean ± SD from n=3-5 independent donors, as represented by individual dots. The GPi induced labeling increase of each compound in stimulated neutrophils were compared with that in unstimulated neutrophils by unpaired t-test, * indicates $p < 0.05$.

d. Labeling patterns of glycolytic intermediates in neutrophils as described in A, but treated with 20uM GPi. n=3-5 independent donors, as represented by individual dots in panel c.

e-f. Dynamic changes of labeling enrichment from U-^{13}C-glucose of indicated glycolytic intermediates, following stimulation with 300μg/mL zymosan A (e) or 1ug/mL LPS (f). Bars and error bars show mean ± SD from n=2 (e) or n=3 (f) independent donors.

Figure 3. Changes of glucose uptake and glycogen cycling upon neutrophil activation.

a. Schematic of glucose uptake, glycogen synthesis, and glycogenolysis. Important enzymes are listed.

b. Glucose consumed from the media within 1 hour by unstimulated neutrophils or neutrophils that are treated with indicated stimuli (300μg/mL zymosan A, 100ng/mL TNFα, or 100nM PMA) or inhibitor (20μM GPi). Bars and error bars show mean ± SD from n=3-4 independent donors,

as represented by individual dots. Statistical analysis was done by unpaired t-test, * indicates $p<0.05$.
c. (Left) Representative flow cytometry result measuring the distribution of GLUT1 level on cell surface within a population of neutrophils that are untreated or treated with indicated stimuli or inhibitor for 30min. (Right) The experiment was repeated with neutrophils isolated from n=4 independent donors (indicated by different markers). Bars and error bars show mean ± SD of quantified mean GLUT1 level from each donor. Statistical analysis was performed by paired t-test.
d-e. Immunoblot analysis of (d) total GLUT1 level and phosphorylated GLUT1 (Ser226), and (e) total PYGL and phosphorylated PYGL (Ser15) in neutrophils treated with indicated stimuli or inhibitor for 30min. Representative blots were shown on the left. The experiment was repeated multiple times with neutrophils isolated for different donors (indicated by individual dots), and quantified results were compiled and shown on the right. Bars and error bars show mean ± SD. Statistical analysis performed by unpaired t-test.
f. Level of glycogen store in human peripheral blood neutrophils that are untreated, treated with GPi (20μM) for 2h, or stimulated with zymosan A (300μg/mL), or LPS (1μg/mL) for 2h. Bars and error bars show mean ± SD from n=4-5 independent donors, as represented by individual dots. p-value determined by paired t-test.
g. Fraction of labeled glycogen after 2hr incubation of neutrophils that are untreated or treated with indicated stimuli or inhibitor in media containing U-^{13}C-glucose. Bars and error bars show mean ± SD from n=3-5 independent donors, as represented by individual dots. p-values were determined by paired t-test.

Figure 4. Increased nutrient utilization upon activation supplies various metabolic pathways
a. Lactate accumulation in spent media of neutrophils that are untreated or treated with GPi or indicated stimuli after 1h. Bars and error bars show mean ± SD from n=3 independent donors, as represented by individual dots. * indicates $p < 0.05$ by unpaired t-test.
b. Relative ribose-5-phosphate (R5P) and ribulose-5-phosphate abundance in neutrophils that are unstimulated or stimulated with 100nM PMA , 300μg/mL zymosan A, 100ng/mL TNFα, or heat inactivated *P. aeruginosa* (HI PsA) for 30min, or with 1μg/mL LPs for 4 hours. Bars and error bars show mean ± SD from n=3 independent donors, as represented by individual dots. p-values were determined by unpaired t-test comparing stimulated condition to unstimulated.
c. Relative R5P abundance (normalized to unstimulated condition) in neutrophils stimulated with zymosan A or PMA for 30min, cultured in media with or without glucose, with or without the treatment of GPi. Bars and error bars show mean ± SD from n=3 independent donors, as represented by individual dots. p-values were determined by unpaired t-test comparing each nutrient perturbed condition (with glucose withdrawal or with GPi treatment) to stimulated neutrophils cultured in standard culture condition (with glucose, with no GPi).
d. Total labeled fraction of TCA cycle metabolites in neutrophils (adhered to tissue culture plate) that are unstimulated or stimulated with 300μg/mL zymosan A after incubation with media containing U-^{13}C-glucose for indicated time.
e. Energy charge in unstimulated neutrophils, or neutrophils stimulated with zymosan A or PMA for 30min, cultured in media with indicated nutrient perturbation (with or without glucose, with or without GPi treatment). Bars and error bars show mean ± SD from n=3 independent donors, as represented by individual dots. p-values were determined by unpaired t-test.

Figure 5. Nutrient dependence of apoptosis, oxidative burst, NET release, and phagocytosis.
a. Percent cells undergone apoptosis (annexin V+) after unstimulated human peripheral blood neutrophils were cultured in indicated media condition for 1 day. Bars and error bars show mean

± SD from n=3 independent donors, as represented by different markers. p-values were determined by unpaired t-test.
b. Oxidative burst induced by 100nM or 20nM PMA or 300ug/mL zymosan A in indicated nutrient conditions. “Control”- standard culture media; “-glucose”- media with no glucose; “+ GPi”, treated with 20uM GPi; “+2DG”—treated with 1mM 2DG; “-glucose+GPi”- cultured in media with no glucose and treated with 20uM GPi; “unstimulated”—neutrophils cultured in standard media without stimuli. The oxidative burst curves shown are a representative result from one neutrophil donor, dot and error bar show mean ± SD from technical replicates (n=8).
c-d. The experiment described in b was repeated with peripheral blood neutrophils isolated from n=3 independent donors, the area under curve (AUC) over the oxidative burst was quantified from results from each donor and shown in c, and the time from stimulation to the peak of oxidative burst was quantified and shown in d. Bars and error bars show mean ± SD. Dots represent result from individual donors. * indicates $p < 0.05$, ns indicate non-significant ($p>0.05$) by unpaired t-test.
e. NET release induced by 100nM PMA stimulation in peripheral blood neutrophils cultured in indicated nutrient conditions, as detailed in b. Dot and error bar show mean ± SD from n=3 independent donors.
f. Phagocytosis of *S. aureus* particles by peripheral blood neutrophils cultured in indicated nutrient conditions, as detailed in b. Curves show representative result. Dot and error bar indicate mean ± SD from n=9 technical replicates. Trends have been confirmed by independent experiments using neutrophils isolated from 3 donors.

Figure 6. Nutrient dependence of neutrophil migration and pathogen killing.
a. Migration of neutrophils through transwell towards 2nM C5a in indicated nutrient condition (with or without glucose, with or without GPi treatment). Bars and error bars show mean ± SD of pooled technical replicates (represented by dots) from 3 individual donors. p-values were determined by unpaired t-test.
b. Representative images of human peripheral blood neutrophils (pre-treated 20uM GPi for 1h before co-incubation with *A. fumigatus* in standard culture media) effectively clustering around and killing *A. fumigatus* hyphae. (Red fluorescent signal is from mCherry expressing *A. fumigatus.* White asterisks indicate neutrophil cluster formation. White arrow indicate fungal cells that have been killed, as indicated by loss of cytosolic RFP signal.)
c. Percent of *A. fumigatus* hyphae with neutrophil clusters (5 or more neutrophils) around after 4 hour co-incubation with untreated primary human neutrophils or neutrophils pretreated with 20uM GPi.
d. Percent of *A. fumigatus* cells remaining after 4 hour co-incubation with untreated primary human neutrophils or neutrophils pretreated with 20uM GPi.
c-d. Bars and error bars show mean ± SD of pooled technical replicates (represented by individual dots) from 2 individual donors (indicated by different colors). Statistical analysis was performed by unpaired t-test.

Supplemental Figure 1.
a. Plasma glucose concentration of 3 participants over the time course of U-^{13}C-glucose infusion.
b-f. Labeling incorporation into plasma lactate, glycerol, glutamine, glutamate, and alanine from U-^{13}C-glucose over the time course of U-13C-glucose infusion. Results show mean ± SD from n=3 independent participants.
g. Labeling incorporation into intracellular TCA cycle metabolites in neutrophils isolated from blood samples 30 or 60 minutes after *in vivo* U-^{13}C-glucose infusion. Results show mean ± SD from n=3 independent participants.
h. Full labeling distribution of glycolytic intermediates in human peripheral blood neutrophils labeled *ex vivo* in media containing U-^{13}C-glucose for 30min, with or without treatment of GPi (20uM).
i. Labeling incorporation into TCA cycle metabolites in peripheral blood neutrophils labeled *ex vivo* in media containing U-^{13}C-glucose for 30 minutes, with or without GPi (20uM) treatment.
j. Average label enrichment of DHAP and glycerol-3-phosphate (G3P) in peripheral blood neutrophils labeled *ex vivo* in media containing U-^{13}C-glucose for 30min, with or without treatment of GPi (20uM).
h-j. Results show mean ± SD from n=3 independent donors.

Supplemental Figure 2.
a. Labeling pattern of UDP-glucose from U-^{13}C-glucose in unstimulated neutrophils with (n=3 donors) or without (n=5 donors) treatment of 20μM GPi, or neutrophils stimulated with 100nM PMA (n=4 donors), 300μg/mL zymosan A (n=6 donors), 100ng/mL TNFα (n=4 donors), or heat inactivated *P. aeruginosa* (HI PsA, 10:1 bacteria: neutrophil) (n=3 donors) for 30 minutes or stimulated with 1ug/mL LPS for 4 hours (n=3 donors). Results show mean ± SD.
b-c. Relative levels of TCA cycle intermediates (b) and ADP/ATP ratio (c) in unstimulated neutrophils or neutrophils stimulated with zymosan A or PMA cultured in media with indicated nutrient perturbation (with or without glucose, with or without GPi treatment). Bars and error bars show mean ± SD from n=3 independent donors, as represented by individual dots.

Supplemental Figure 3.
a. Viability of unstimulated neutrophils over a course of 5h when cultured in indicated media condition (with or without glucose, with or without 20μM GPi treatment). Control is standard RPMI media-based culture condition. 'Live cells' are the cells that are negative of both Cytotoxic and annexin V stain. Mean ± SD from n=3 independent donors.
b. Percent of live cells after unstimulated neutrophils were cultured in indicated media condition for 1 day (23-24h). Bars and error bars show mean ± SD from n=3 independent donors, as represented by different markers.

Supplemental Figure 4.
a. Labeling pattern of intracellular glycolytic intermediates following 4-hour incubation in U-^{13}C-glucose media in neutrophils that are untreated, treated with 20uM GPi throughout the duration of labeling, or pre-treated with 20uM GPi for 1hr prior to labeling in media containing no GPi. Bars and error bars show mean ± SD from n=3 technical replicates.
b. Migration of neutrophils through transwell towards 2nM C5a. Cells were untreated (-GPi), pretreated with GPi for 30 minutes prior to addition to transwell without GPi for migration assay (GPi pretreat), or treated with 20uM GPi throughout the duration of migration assay (GPi retain). Bars and error bars show mean ± SD from n=3 technical replicates (indicated by individual dots). Statistical analysis was performed by unpaired t-test.

Methods

In vivo isotopic tracing

Healthy adults with no previous history of diabetes received infusions of U-13C-glucose after informed consent was obtained following the protocol approved by the UW IRB (2020-1008-CP001). Sterile and endotoxin-free U-13C-glc was administered as a bolus of 8 grams over 10 minutes followed by an 8 g/hour infusion over 2 hours. Neutrophils were isolated from peripheral blood collected prior to infusion and at 30 and 60 minutes following the start of infusion. Neutrophils were pelleted by spinning at 500 x g for 2 minutes. Metabolites were extracted from plasma and neutrophil pellets by addition of LC-MS grade 40:40:40 acetonitrile/methanol/water (40:40:20 v:v:v). Samples were spun at 20,627*g* for 5 min at 4 C to remove any insoluble debris prior to analysis on LC-MS (see below for details).

Due to poor ionization of glycerol, it was first enzymatically converted into glycerol-3-phosphate prior to analysis on LC-MS[49]. Briefly, plasma samples were incubated with glucokinase (Sigma-Aldrich G6278) for 10 minutes at room temperature in the following buffer (5mM Tris-HCl, 50mM NaCl, 10mM MgCl2, 5mM ATP). After incubation, reaction was quenched with LC-MS grade 40:40:40 acetonitrile/methanol/water +0.1% formic acid (40:40:20 v:v:v) and neutralized with 15% ammonium bicarbonate. Samples were spun at 16,000 x g for 10 minutes at 4oC prior to analysis on LC-MS.

Isolation, culture and stimulation of human peripheral blood neutrophils

Human neutrophils were isolated from peripheral blood freshly collected from healthy donors, following the protocol approved by the University of Wisconsin Institutional Review Board (protocol no. 2019-1031-CP001). Informed consent was obtained from all participants. Neutrophils were purified using the MACSxpress Whole Blood Neutrophil Isolation Kit (Miltenyi Biotec, no. 130-104-434) followed by erythrocyte depletion (Miltenyi Biotec, no. 130-098-196) according to the manufacturer's instructions. Neutrophils were spun down at 300g for 5 min, resuspended in RPMI 1640 (VWR, no. VWRL0106-0500) supplemented with 5 mM L-glutamine (Fisher Scientific, no. BP379-100) and 0.1% Human Serum Albumin (Lee Biosolutions, no. 101-15) and kept at 37oC in incubators under 5% CO2. For experiments without glucose the media was as follows: RPMI 1640 (VWR, no. IC091646854) supplemented with 5 mM L-glutamine (Fisher Scientific, no. BP379-100) and 0.1% Human Serum Albumin (Lee Biosolutions, no. 101-15). Purity of isolated cells was verified by flow cytometry as previously established[7].

For stimulation, between 1.5 and 3 million neutrophils were aliquoted into 1.5-ml Eppendorf tubes. Stimulation by PMA (Cayman Chemical, no. 10008014) was provided to cell suspensions at the indicated concentrations in each experiment. *P. aeruginosa* (PAK strain) were cultured overnight, sub-cultured until mid-exponential phase then opsonized in human serum (Sigma-Aldrich, no. H4522) for 30 min. Opsonized PsA was spun down at 10,000g for 1 min, washed and resuspended in PBS, then heat inactivated at 95oC for 5 minutes before addition to neutrophil suspension at 10:1 bacterial/neutrophil cells. Zymosan A was opsonized by incubation with human serum (Sigma-Aldrich, no. H4522) at 37 °C for 30 min, washed twice and resuspended in PBS then added to neutrophils at the indicated concentration for stimulation. TNF-α (R&D systems, no. 210-TA-020) was dissolved in PBS to make a stock solution and added to neutrophils for stimulation. LPS (E. coli O111:B4, Sigma) was dissolved in PBS to make a stock solution then sonicated in a water bath for 10 minutes prior to addition to cell suspensions. In experiments involving inhibitors, glycogen phosphorylase inhibitor (GPi) (2-chloro-4,5-difluoro-N-[[[2-methoxy-5-[[(methylamino)carbonyl]amino]phenyl]amino]carbonyl]-benzamide; Cayman Chemical, no. 17578) at 10 or 20uM was added concurrently with stimulation (unless otherwise noted) at the indicated concentrations.

Culture of HL-60 cells

HL-60 cells were cultured in RPMI with 5 mM glutamine, 25 mM HEPES, 15% fetal bovine serum (FBS) and 1% penicillin/streptomycin. To differentiate HL-60 to a neutrophil-like state, cells were transferred to differentiation medium (RPMI with 1.3% DMSO, 5 mM glutamine, 25 mM HEPES, 9% FBS and 1% penicillin/streptomycin) for 6 days, with medium change on day 3. After 6 days, differentiated neutrophil-like cells were verified by flow cytometry as previously established[7] and were used in experiments in culture media without DMSO.

***Ex vivo* and *in vitro* isotopic tracing**

For all experiments involving the stable isotope tracer U-^{13}C-glucose (Cambridge Isotope, no. CLM-1396), isotopically labeled glucose was substituted for unlabeled glucose at the same concentration in RPMI culture medium. Natural ^{13}C abundance was corrected from raw data. For *ex vivo* isotopic labeling experiments with stimulated neutrophils (PMA, Zymosan A, TNF, and HI PsA) U-^{13}C-glucose media was substituted in culture media for unlabeled glucose for indicated time. The exception was LPS stimulation, neutrophils were stimulated with 1ug/mL LPS for 3 hours in unlabeled glucose media prior to switching to U-13C-gluose media for an additional hour for a total of 4 hour stimulation.

Metabolomics

To extract intracellular metabolites, culture medium was removed and neutrophils were immediately washed with PBS. Each 2 million pelleted neutrophils were extracted with 150 µl of cold liquid chromatography–mass spectrometry (LC–MS)-grade acetonitrile/methanol/water (40:40:20 v:v:v), and samples were spun at 20,627*g* for 5 min at 4 C to remove any insoluble debris. To analyze extracellular metabolites, spent media samples were extracted with 4× volume of LC–MS grade methanol, and protein pellets were removed by centrifugation. Supernatant containing small molecules was further diluted with either LC–MS grade H2O or acetonitrile/methanol/water (40:40:20 v:v:v) for different LC–MS analysis methods. Soluble metabolite samples were analyzed with a Thermo Q-Exactive mass spectrometer coupled to a Vanquish Horizon Ultra-High Performance Liquid Chromatograph, using the following two analytical methods. (1) Samples in extraction solvent were directly loaded on to LC–MS, then separated on a 2.1 × 150mm Xbridge BEH Amide (2.5 µm) Column (Waters) using a gradient of solvent A (95% H_2O, 5% ACN, 20 mM NH_4AC, 20 mM NH_4OH) and solvent B (20% H_2O, 80% ACN, 20 mM NH_4AC, 20 mM NH_4OH). The gradient used was 0 min, 100% B; 3 min, 100% B; 3.2 min, 90% B; 6.2 min, 90% B; 6.5 min, 80% B; 10.5 min, 80% B; 10.7 min, 70% B; 13.5 min, 70% B; 13.7 min, 45% B; 16 min, 45% B; 16.5 min, 100% B; 22 min, 100% B. The flow rate was 0.3 ml min^{-1} and column temperature 30 °C. Analytes were measure by MS using full scan. (2) Samples were dried under N_2 flow and resuspended in LC–MS-grade water as loading solvent. Metabolites were separated on a 2.1 × 100mm, 1.7 µM Acquity UPLC BEH C18 Column (Waters) with a gradient of solvent A (97:3 H_2O/methanol, 10 mM TBA, 9 mM acetate, pH 8.2) and solvent B (100% methanol). The gradient was: 0 min, 5% B; 2.5 min, 5% B; 17 min, 95% B; 21 min, 95% B; 21.5 min, 5% B. Flow rate was 0.2 ml min^{-1}. Data were collected with full scan. Identification of metabolites reported here was based on exact *m/z* and retention time that were determined with chemical standards. Data were collected with Xcalibur 4.0 software and analyzed with Maven. Due to a limited cell number from each neutrophil donor not all simulation conditions could be done on one donor, so for determining metabolite abundance, LC-MS data was normalized to resting condition per experiment.

To determine energy charge, relative metabolite abundance of AMP, ADP, and ATP was measured by ion count in LC-MS analysis. Energy charge is calculated based on *Equation 1*.

Equation 1. $$Energy\ Charge = \frac{[ATP]+0.5[ADP]}{[ATP]+[AMP]+[ADP]}$$

Flow cytometry

To measure external GLUT1 5x105 neutrophils were aliquoted. Following 15 minutes of Fc-block, primary antibodies were added and incubated at room temperature for 30 minutes. Primary antibodies: CD11b (PE) (Biolegend, no. 301305), GLUT-1 (FITC) (Alomone Labs, AGT-041-F), Ghost Dye Violet 450 (Tonbo, no.13-0863). After staining, cells were pelleted at 500 x g for 2 minutes and fixed in 0.4% paraformaldehyde at room temperature for 10 minutes. Cells were pelleted at 500 x g for 2 minutes and resuspended in PBS for flow cytometric analysis. Samples were acquired on an Attune NxT V6 (ThermoFisher). Analysis was completed using FlowJo software. Cells were gated for viability and CD11B expression prior to GLUT1 expression gating.

Immunoblotting

Approximately 4 million cells were harvested with Laemmli lysis buffer with phosphatase inhibitor (Thermo Scientific, no. A32957) and HALT protease inhibitor (Thermo Scientific, no. 78425). Proteins of interest were probed with the following antibodies in TBS-T buffer with 5% BSA. Primary antibodies: PYGL (abcam, ab198268), phospho(S15)-PYGL (abcam, ab227043), GLUT1 (Alomone Labs, AGT-041), P-GLUT1 (Millipore Sigma, ABN991), B-actin (Cell Signaling, no. 4967); and secondary antibodies: Goat-anti-rabbit 800 (LI-COR, no. 925-32211), Goat-anti-mouse 680 (LI-COR, no. 925-68070). Membranes were imaged with a Li-Cor Odyssey ClX and quantified using ImageStudio Lite software

Glycogen Assay

Approximately 3 million cells were aliquoted and treated with various stimuli and/or inhibitors. After indicated incubation at 37C cells were pelleted at 300 x g for 2 minutes. Cells were lysed with ice cold H2O and boiled at 100oC for 15 minutes. Mixture was spun at 1000 x g for 10 minutes at 4oC to pellet cell debris. To quantify total glycogen level from the supernatant the glycogen assay kit (Cayman Chemical, no. 700480) was used. To quantify glycogen synthesis from extracellular glucose, samples were incubated in media containing U-13C-glucose. After incubation and glycogen extraction detailed above, glycogen was hydrolyzed with hydrolysis enzyme (Cayman Chemical, no. 700483) at 37C for 30 minutes. Protein was crashed out by addition of 900ul LC-MS grade acetonitrile. Samples were spun at 20,627*g* for 5 min at 4 C and 850ul of supernatant was transferred to new tube and dried under nitrogen stream. Samples were resuspended in LCMS water prior to injection on LC-MS.

Cell viability assay

Neutrophils were plated in culture wells precoated with Cell-Tak (Corning, no. 354240) at 5 × 10^4 cells per well in RPMI media with 11mM glucose or without glucose with 0.1% human serum albumin (HSA). 20uM GPi or DMSO control was added to appropriate wells and the plate incubated at 37C for 1 hour. Prior to imaging Cytotox Green (Sartorius 4633) and Annexin V (Sartorius 4641) dyes were added per manufacturer recommendation. Images were taken every 30-60 minutes for 24 hours. Images were analyzed using IncuCyte S3 Basic Analysis software.

Assay for oxidative burst

Oxidative burst was measured by stimulation-induced oxygen consumption rate (OCR) using a XF-96e extracellular flux analyzer (Agilent) following a protocol developed by Seahorse[50]. To

attach neutrophils at the bottom of assay plates (Seahorse Bioscience), neutrophils were plated in culture wells precoated with Cell-Tak (Corning, no. 354240) at 4 × 104 cells per well, spun at 200g for 1 min with minimal acceleration/deceleration then incubated for 1 h at 37 °C. Assays were performed in regular neutrophil culture media (RPMI 1640 medium supplemented with 0.1% human serum albumin) or RPMI without glucose. Inhibitors GPi or vehicle control were added just before starting the assay. After several baseline OCR measurements, biochemical stimulant was injected through the injection ports to induce oxidative burst, and the OCR was continuously monitored throughout the course of oxidative burst.

NET release assay

NET release was quantified by increase in extracellular DNA over time following a previously developed protocol[51]. Briefly, neutrophils were plated at 4 × 10^4 cells per well in a 96-well tissue culture plate precoated with Cell-Tak (Corning, no. 354240) and spun at 200g for 1 min with minimal acceleration/deceleration. Cytotox Green Reagent (IncuCyte, no. 4633) was added to culture media at 1:4,000 to stain extracellular DNA, and images were captured every 10–30 min after stimulation using an IncuCyte live cell imager under standard culture conditions (37 °C, 5% CO2). The fluorescent area outside of cells, which indicates NET, was quantified by image analysis using IncuCyte S3 Basic Analysis software. NET release represented by the ratio of green fluorescence relative to phase area.

Phagocytosis assay

Phagocytosis was quantified by signal from pHrodo *S. aureus* bioparticles® (Sartorius, no. 4619) which increase fluorescence upon phagocytosis due to the acidic environment of phagosome. Briefly, neutrophils were plated at 4 × 104 cells per well in a 96-well tissue culture plate precoated with Cell-Tak (Corning, no. 354240) and spun at 200g for 1 min with minimal acceleration/deceleration. Neutrophils were either plated in standard RPMI or pretreated with GPi or plated in no glucose RPMI media. pHrodo *S. aureus* bioparticles® (Sartorius, no. 4619) were added and images were captured every 15 minutes under standard culture conditions (37 °C, 5% CO2). The fluorescent area was quantified using IncuCyte S3 Basic Analysis software and normalized to phase area

Neutrophil migration toward C5a

Migration assays were performed using transwell inserts with 3 µm pores (Corning 3415). Isolated primary neutrophils were rested for 30 minutes in RPMI 1640 containing 11mM glucose and 0.1% HSA. After the rest period, cells were pre-treated for 30 minutes with experimental media. Then 2e5 cells were placed into loading control wells or transwells and migrated towards 2 nM C5a (biotechne, 2037-C5). Images were taken throughout the migration process and cells migrating to the bottom of each well were quantified using IncuCyte S3 Basic Analysis software. Cell migration plateaued at 2-hours, therefore the 2-hour timepoint was used to quantify migration. The number of cells migrated were normalized to the control group (11 mM Glucose, DMSO) and corrected for cell loading.

Fungal control and neutrophil recruitment

To assess neutrophil/fungal interactions, A. fumigatus strain CEA10-RFP (TDGC1.2) was grown on glucose minimal media (GMM) at 37°C in the dark for 3 days prior to the experimental start date to induce asexual conidiation. Following incubation, fungal spores were collected in approximately 25ml of a 0.01% Tween 20 solution using an L-spreader and filtered through a 0.4µm mesh filter (Fischer Scientific) into a 50ml conical tube. A 5ml aliquot was then transferred to a new tube, centrifuged at 800rpm for 5 minutes and then resuspended in GMM. Fungal spores were then quantified via hemocytometer and diluted to a final concentration of 4

x 103 cells/ml in GMM. Following dilution, 100μl of the spore suspension was added to the appropriate number of wells in a 96-well clear, flat bottom plate and left to incubate at 37°C + 5% CO2 for 8 hours, or until germlings appeared.
Roughly two hours prior to the end of the spore incubation, primary human neutrophils were collected as previously described and diluted to a cell concentration of 4 x 105 cells/ml in RPMI + 0.1% human serum albumin. Following dilution, 20μM of glycerol phosphorylase inhibitor (GPI) (Caymen Chemicals) or an appropriate volume of DMSO solvent control was added to the neutrophil stocks and incubated at 37C for 1 hour before being replaced with RPMI + 0.1% human serum albumin. After germling development, the media was removed from all wells in the 96-well plate and replaced with 100μl of the neutrophil suspension. The plate was then immediately taken to a Nikon Eclipse Ti inverted microscope with a preheated chamber set to 37°C and initial images, denoted as time 0 (T0), were taken for all wells. All locations imaged in the plate were tracked in the NIS Element software package connected to the microscope. Following image acquisition, the plate was incubated for 4 hours at 37°C + 5% CO2. After 4 hours, the plate was removed and imaged at the same locations captured at the start of the experiment (T4). Images were then analyzed for the presence/absence of red hyphal fluorescence between T4 and T0, and for the formation of neutrophil clusters around hyphal cells that were present at the T0 time point.
For all conditions, three biological replicates with one to three technical replicates were performed using three separate donors. Statistical differences were assessed via a student's t-test or a non-parametric Kruskal-Wallis test (GraphPad Prism, v7.0c software).

Conflict of Interest Statement

The authors declare no conflict of interest.

Acknowledgement

The authors thank Mark Zhang, Mariah Endres, Mitch Howard, and Christina Sheehan for assistance and coordination related to the in vivo infusion study. The authors thank Matt Stefely for assistance in figure editing and Alicia Willians for text editing. This work is supported by NIH grant R35GM147014 (J.F.), R35GM118027 (A.H.), and UW2020 Initiative award AAH8454 provided by the University of Wisconsin - Madison Office of the Vice Chancellor for Research and Graduate Education with funding from the Wisconsin Alumni Research Foundation (J.F., S.M.S, and C.D.F.). Student support was provided in part by T32GM140935 (J.L., N.L.A.), TL1TR002375 (J.L.), and UL1TR002373 (J.L.).

References

1. Jeon, J.-H., Hong, C.-W., Kim, E. Y. & Lee, J. M. Current Understanding on the Metabolism of Neutrophils. *Immune Netw.* **20**, e46 (2020).
2. Kumar, S. & Dikshit, M. Metabolic Insight of Neutrophils in Health and Disease. *Front. Immunol.* **10**, (2019).
3. Borregaard, N. & Herlin, T. Energy Metabolism of Human Neutrophils during Phagocytosis. *J. Clin. Invest.* **70**, 550–557 (1982).
4. Fossati, G. *et al.* The Mitochondrial Network of Human Neutrophils: Role in Chemotaxis, Phagocytosis, Respiratory Burst Activation, and Commitment to Apoptosis. *J. Immunol.* **170**, 1964–1972 (2003).
5. Maianski, N. A. *et al.* Functional characterization of mitochondria in neutrophils: a role restricted to apoptosis. *Cell Death Differ.* **11**, 143–153 (2004).
6. Sadiku, P. *et al.* Neutrophils Fuel Effective Immune Responses through Gluconeogenesis and Glycogenesis. *Cell Metab.* **33**, 411-423.e4 (2021).
7. Britt, E. C. *et al.* Switching to the cyclic pentose phosphate pathway powers the oxidative burst in activated neutrophils. *Nat. Metab.* **4**, 389–403 (2022).
8. Azevedo, E. P. *et al.* A Metabolic Shift toward Pentose Phosphate Pathway Is Necessary for Amyloid Fibril- and Phorbol 12-Myristate 13-Acetate-induced Neutrophil Extracellular Trap (NET) Formation*. *J. Biol. Chem.* **290**, 22174–22183 (2015).
9. Ghergurovich, J. M. *et al.* A small molecule G6PD inhibitor reveals immune dependence on pentose phosphate pathway. *Nat. Chem. Biol.* **16**, 731–739 (2020).
10. Siler, U. *et al.* Severe glucose-6-phosphate dehydrogenase deficiency leads to susceptibility to infection and absent NETosis. *J. Allergy Clin. Immunol.* **139**, 212-219.e3 (2017).
11. Macintyre, A. N. *et al.* The Glucose Transporter Glut1 Is Selectively Essential for CD4 T Cell Activation and Effector Function. *Cell Metab.* **20**, 61–72 (2014).

12. Thwe, P. M. *et al.* Cell-Intrinsic Glycogen Metabolism Supports Early Glycolytic Reprogramming Required for Dendritic Cell Immune Responses. *Cell Metab.* **26**, 558-567.e5 (2017).
13. Zhang, H. *et al.* TCR activation directly stimulates PYGB-dependent glycogenolysis to fuel the early recall response in CD8+ memory T cells. *Mol. Cell* **82**, 3077-3088.e6 (2022).
14. Huang, J.-B., Kindzelskii, A. L. & Petty, H. R. Hexokinase translocation during neutrophil activation, chemotaxis, and phagocytosis: disruption by cytochalasin D, dexamethasone, and indomethacin. *Cell. Immunol.* **218**, 95–106 (2002).
15. Weisdorf, D. J., Craddock, P. R. & Jacob, H. S. Granulocytes utilize different energy sources for movement and phagocytosis. *Inflammation* **6**, 245–256 (1982).
16. Tan, A. S., Ahmed, N. & Berridge, M. V. Acute Regulation of Glucose Transport After Activation of Human Peripheral Blood Neutrophils by Phorbol Myristate Acetate, fMLP, and Granulocyte-Macrophage Colony-Stimulating Factor. *Blood* **91**, 649–655 (1998).
17. Khatib-Massalha, E. *et al.* Lactate released by inflammatory bone marrow neutrophils induces their mobilization via endothelial GPR81 signaling. *Nat. Commun.* **11**, 3547 (2020).
18. Krysa, S. J. & Allen, L.-A. H. Metabolic Reprogramming Mediates Delayed Apoptosis of Human Neutrophils Infected With Francisella tularensis. *Front. Immunol.* **13**, (2022).
19. Ohms, M. *et al.* Enhanced Glycolysis Is Required for Antileishmanial Functions of Neutrophils Upon Infection With Leishmania donovani. *Front. Immunol.* **12**, (2021).
20. Li, D.-D. *et al.* Fungal sensing enhances neutrophil metabolic fitness by regulating antifungal Glut1 activity. *Cell Host Microbe* **30**, 530-544.e6 (2022).
21. Rice, C. M. *et al.* Tumour-elicited neutrophils engage mitochondrial metabolism to circumvent nutrient limitations and maintain immune suppression. *Nat. Commun.* **9**, 5099 (2018).
22. Amini, P. *et al.* Neutrophil extracellular trap formation requires OPA1-dependent glycolytic ATP production. *Nat. Commun.* **9**, 2958 (2018).

23. Kaymak, I. *et al.* Carbon source availability drives nutrient utilization in CD8+ T cells. *Cell Metab.* **34**, 1298-1311.e6 (2022).
24. Cantor, J. R. *et al.* Physiologic Medium Rewires Cellular Metabolism and Reveals Uric Acid as an Endogenous Inhibitor of UMP Synthase. *Cell* **169**, 258-272.e17 (2017).
25. Faubert, B., Tasdogan, A., Morrison, S. J., Mathews, T. P. & DeBerardinis, R. J. Stable isotope tracing to assess tumor metabolism in vivo. *Nat. Protoc.* **16**, 5123–5145 (2021).
26. Kim, I.-Y., Suh, S.-H., Lee, I.-K. & Wolfe, R. R. Applications of stable, nonradioactive isotope tracers in in vivo human metabolic research. *Exp. Mol. Med.* **48**, e203–e203 (2016).
27. Fernández-García, J., Altea-Manzano, P., Pranzini, E. & Fendt, S.-M. Stable Isotopes for Tracing Mammalian-Cell Metabolism In Vivo. *Trends Biochem. Sci.* **45**, 185–201 (2020).
28. Faubert, B. *et al.* Lactate Metabolism in Human Lung Tumors. *Cell* **171**, 358-371.e9 (2017).
29. Linden, C. V. & Corbet, C. Killing two birds with one stone: Blocking the mitochondrial pyruvate carrier to inhibit lactate uptake by cancer cells and radiosensitize tumors. *Mol. Cell. Oncol.* **5**, e1465016 (2018).
30. TeSlaa, T. *et al.* The Source of Glycolytic Intermediates in Mammalian Tissues. *Cell Metab.* **33**, 367-378.e5 (2021).
31. Ma, E. H. *et al.* Metabolic Profiling Using Stable Isotope Tracing Reveals Distinct Patterns of Glucose Utilization by Physiologically Activated CD8+ T Cells. *Immunity* **51**, 856-870.e5 (2019).
32. Maratou, E. *et al.* Glucose transporter expression on the plasma membrane of resting and activated white blood cells. *Eur. J. Clin. Invest.* **37**, 282–290 (2007).
33. Lee, E. E. *et al.* A Protein Kinase C Phosphorylation Motif in GLUT1 Affects Glucose Transport and is Mutated in GLUT1 Deficiency Syndrome. *Mol. Cell* **58**, 845–853 (2015).
34. Sergeant, S. & McPhail, L. C. Opsonized zymosan stimulates the redistribution of protein kinase C isoforms in human neutrophils. *J. Immunol. Baltim. Md 1950* **159**, 2877–2885 (1997).

35. Kilpatrick, L. E., Sun, S., Li, H., Vary, T. C. & Korchak, H. M. Regulation of TNF-induced oxygen radical production in human neutrophils: role of δ-PKC. *J. Leukoc. Biol.* **87**, 153–164 (2010).
36. Schoen, T. J. *et al.* Aspergillus fumigatus transcription factor ZfpA regulates hyphal development and alters susceptibility to antifungals and neutrophil killing during infection. *PLOS Pathog.* **19**, e1011152 (2023).
37. Kedia-Mehta, N. & Finlay, D. K. Competition for nutrients and its role in controlling immune responses. *Nat. Commun.* **10**, 2123 (2019).
38. Stegenga, M. E. *et al.* Hyperglycemia enhances coagulation and reduces neutrophil degranulation, whereas hyperinsulinemia inhibits fibrinolysis during human endotoxemia. *Blood* **112**, 82–89 (2008).
39. Wang, L. *et al.* Hyperglycemia Induces Neutrophil Extracellular Traps Formation Through an NADPH Oxidase-Dependent Pathway in Diabetic Retinopathy. *Front. Immunol.* **9**, (2019).
40. Wong, S. L. *et al.* Diabetes primes neutrophils to undergo NETosis, which impairs wound healing. *Nat. Med.* **21**, 815–819 (2015).
41. Kim, S. Y., Jun, H. S., Mead, P. A., Mansfield, B. C. & Chou, J. Y. Neutrophil stress and apoptosis underlie myeloid dysfunction in glycogen storage disease type Ib. *Blood* **111**, 5704–5711 (2008).
42. Jun, H. S., Weinstein, D. A., Lee, Y. M., Mansfield, B. C. & Chou, J. Y. Molecular mechanisms of neutrophil dysfunction in glycogen storage disease type Ib. *Blood* **123**, 2843–2853 (2014).
43. Cheung, Y. Y. *et al.* Impaired neutrophil activity and increased susceptibility to bacterial infection in mice lacking glucose-6-phosphatase-beta. *J. Clin. Invest.* **117**, 784–793 (2007).
44. Jun, H. S. *et al.* Lack of glucose recycling between endoplasmic reticulum and cytoplasm underlies cellular dysfunction in glucose-6-phosphatase-beta-deficient neutrophils in a congenital neutropenia syndrome. *Blood* **116**, 2783–2792 (2010).

45. Kim, S. Y., Chen, L.-Y., Yiu, W. H., Weinstein, D. A. & Chou, J. Y. Neutrophilia and elevated serum cytokines are implicated in glycogen storage disease type Ia. *FEBS Lett.* **581**, 3833–3838 (2007).
46. Hirschfeld, J., White, P. C., Milward, M. R., Cooper, P. R. & Chapple, I. L. C. Modulation of Neutrophil Extracellular Trap and Reactive Oxygen Species Release by Periodontal Bacteria. *Infect. Immun.* **85**, e00297-17 (2017).
47. Patel, C. H., Leone, R. D., Horton, M. R. & Powell, J. D. Targeting metabolism to regulate immune responses in autoimmunity and cancer. *Nat. Rev. Drug Discov.* **18**, 669–688 (2019).
48. Pålsson-McDermott, E. M. & O'Neill, L. A. J. Targeting immunometabolism as an anti-inflammatory strategy. *Cell Res.* **30**, 300–314 (2020).
49. Chiles, E. *et al.* Fast LC-MS Quantitation of Glucose and Glycerol Via Enzymatic Derivatization. *Anal. Biochem.* **575**, 40–43 (2019).
50. Swain, P., Romero, N. & Dranka, B. P. Modulation of oxidative burst with exposure to cytokines in neutrophil cell activation. in.
51. A High-Throughput Real-Time Imaging Technique To Quantify NETosis and Distinguish Mechanisms of Cell Death in Human Neutrophils | The Journal of Immunology. https://www.jimmunol.org/content/200/2/869.long.

Figure 1

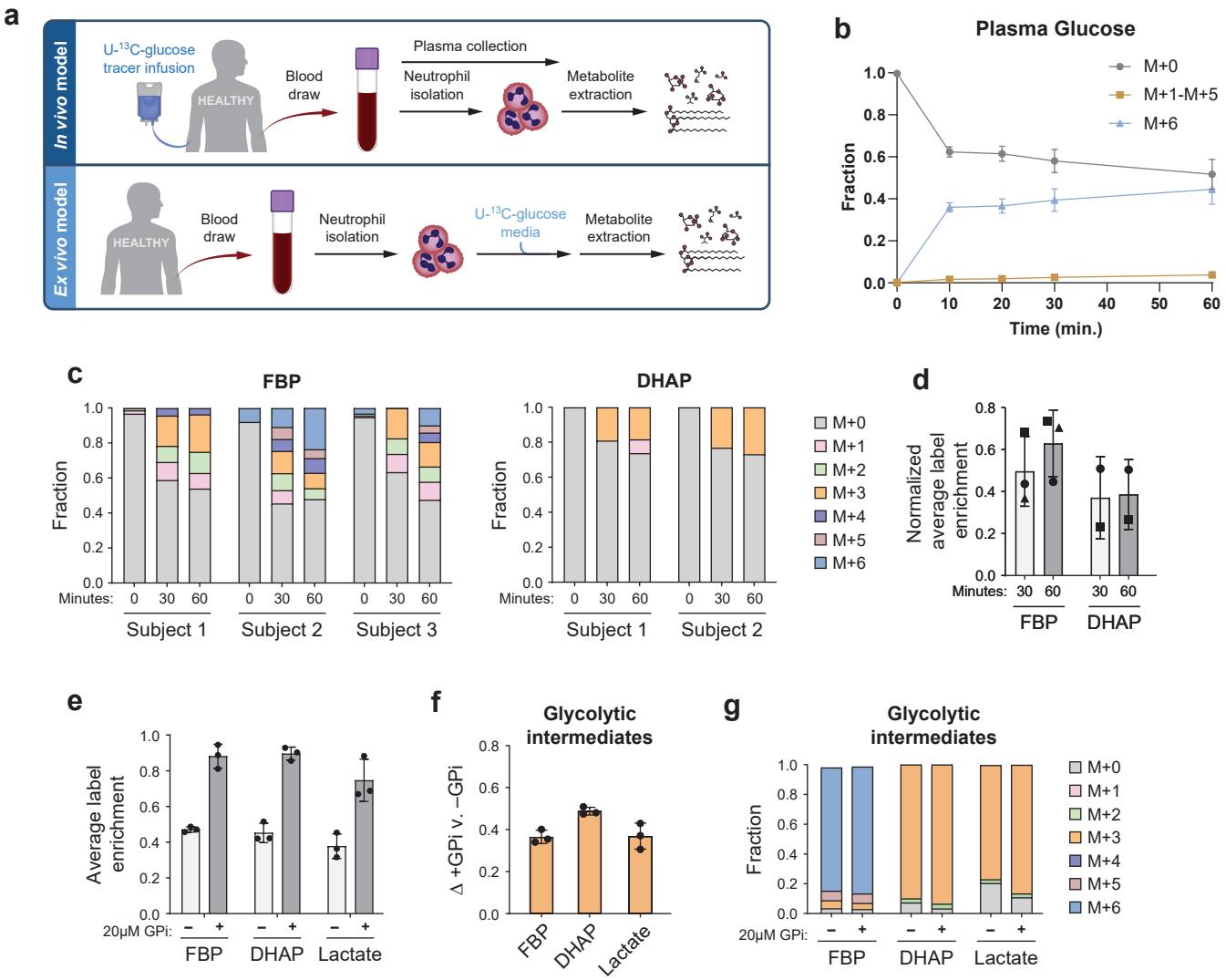
a
In vivo model
U-13C-glucose tracer infusion
HEALTHY
Blood draw
Plasma collection
Neutrophil isolation
Metabolite extraction
Ex vivo model
HEALTHY
Blood draw
Neutrophil isolation
U-13C-glucose media
Metabolite extraction
b
Plasma Glucose
M+0
M+1-M+5
M+6
Fraction
Time (min.)
c
FBP
DHAP
Fraction
Minutes:
Subject 1
Subject 2
Subject 3
M+0
M+1
M+2
M+3
M+4
M+5
M+6
d
Normalized average label enrichment
Minutes:
FBP
DHAP
e
Average label enrichment
20μM GPi:
FBP
DHAP
Lactate
f
Glycolytic intermediates
Δ +GPi v. –GPi
FBP
DHAP
Lactate
g
Glycolytic intermediates
Fraction
20μM GPi:
FBP
DHAP
Lactate
M+0
M+1
M+2
M+3
M+4
M+5
M+6

Figure 2

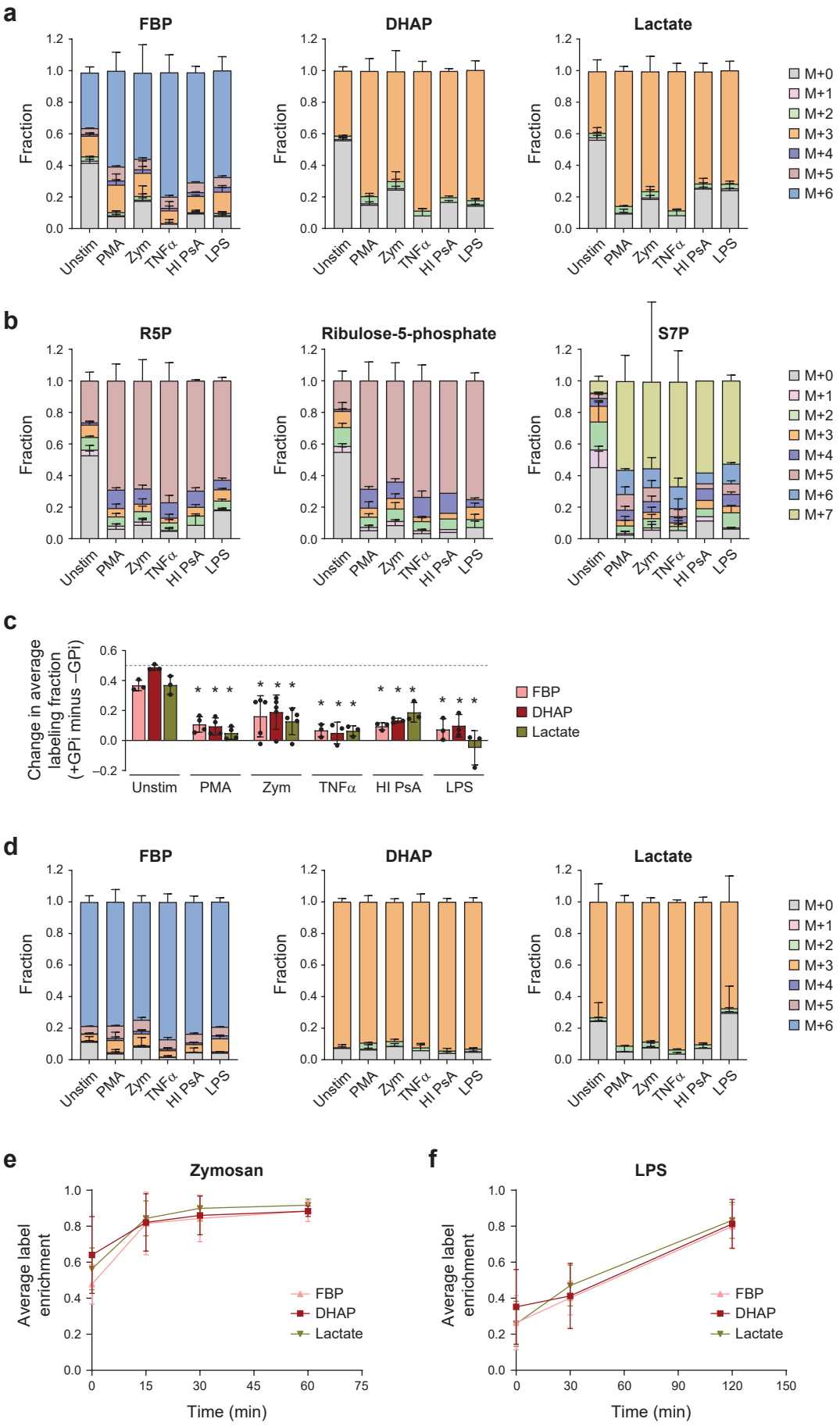
a
FBP
DHAP
Lactate
Fraction
Unstim
PMA
Zym
TNFα
HI PsA
LPS
M+0
M+1
M+2
M+3
M+4
M+5
M+6
b
R5P
Ribulose-5-phosphate
S7P
M+7
c
Change in average labeling fraction (+GPi minus –GPi)
FBP
DHAP
Lactate
d
e
Zymosan
Average label enrichment
Time (min)
f
LPS

Figure 3

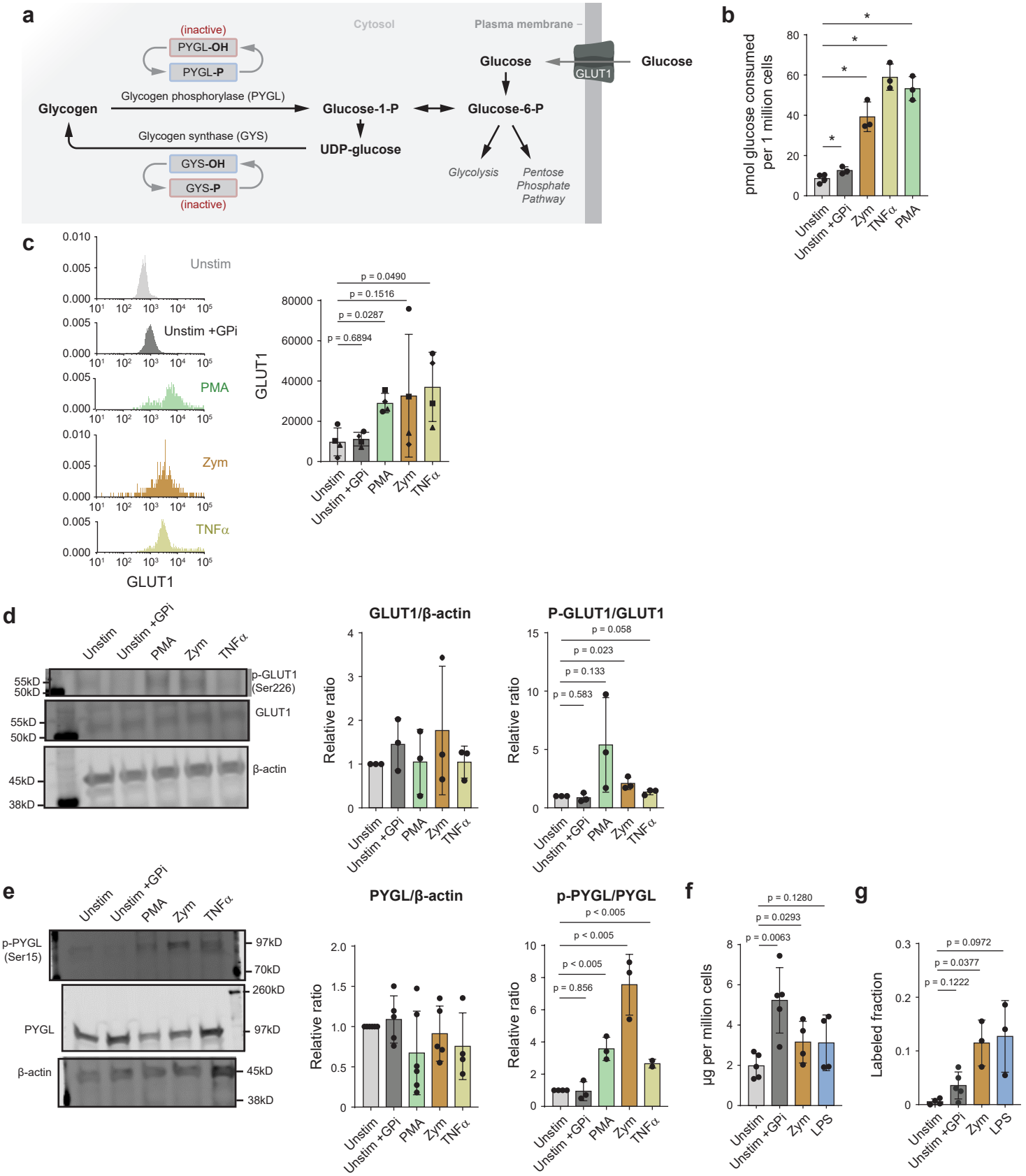
a
Cytosol
Plasma membrane
(inactive)
PYGL-OH
PYGL-P
Glycogen
Glycogen phosphorylase (PYGL)
Glucose-1-P
Glucose-6-P
Glucose
GLUT1
Glucose
Glycogen synthase (GYS)
UDP-glucose
GYS-OH
GYS-P
(inactive)
Glycolysis
Pentose Phosphate Pathway
b
pmol glucose consumed per 1 million cells
Unstim
Unstim +GPi
Zym
TNFα
PMA
c
Unstim
Unstim +GPi
PMA
Zym
TNFα
GLUT1
p = 0.0490
p = 0.1516
p = 0.0287
p = 0.6894
d
Unstim
Unstim +GPi
PMA
Zym
TNFα
55kD
50kD
p-GLUT1 (Ser226)
GLUT1
β-actin
45kD
38kD
GLUT1/β-actin
P-GLUT1/GLUT1
Relative ratio
p = 0.058
p = 0.023
p = 0.133
p = 0.583
e
p-PYGL (Ser15)
PYGL
β-actin
97kD
70kD
260kD
45kD
38kD
PYGL/β-actin
p-PYGL/PYGL
p < 0.005
p = 0.856
f
μg per million cells
p = 0.1280
p = 0.0293
p = 0.0063
LPS
g
Labeled fraction
p = 0.0972
p = 0.0377
p = 0.1222

Figure 4

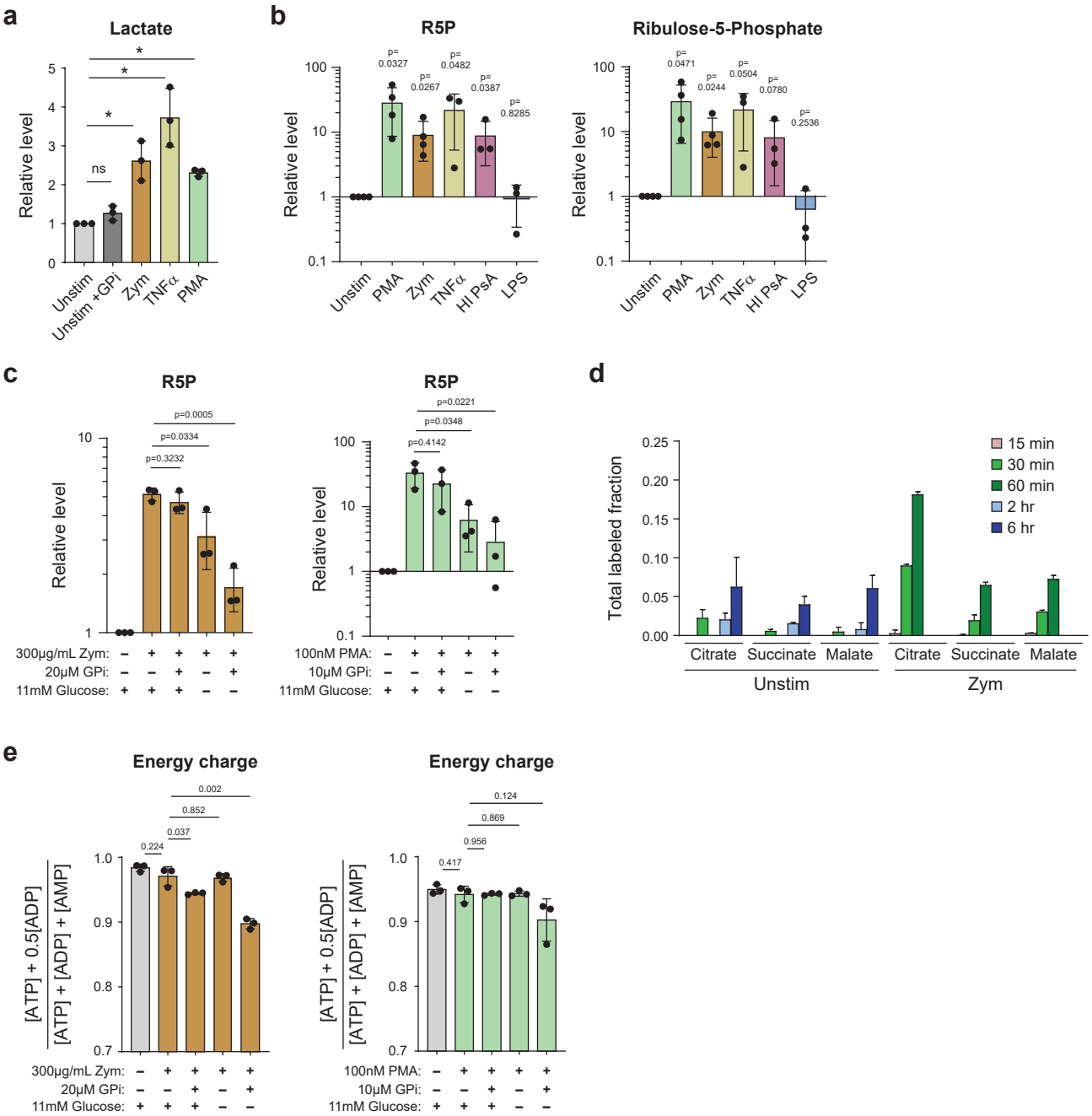
a
Lactate
Relative level
ns
*
Unstim
Unstim +GPi
Zym
TNFα
PMA
b
R5P
Ribulose-5-Phosphate
p= 0.0327
p= 0.0267
p= 0.0482
p= 0.0387
p= 0.8285
p= 0.0471
p= 0.0244
p= 0.0504
p= 0.0780
p= 0.2536
Unstim
PMA
Zym
TNFα
HI PsA
LPS
c
R5P
p=0.0005
p=0.0334
p=0.3232
p=0.0221
p=0.0348
p=0.4142
300μg/mL Zym:
20μM GPi:
11mM Glucose:
100nM PMA:
10μM GPi:
d
Total labeled fraction
15 min
30 min
60 min
2 hr
6 hr
Citrate
Succinate
Malate
Unstim
Zym
e
Energy charge
[ATP] + 0.5[ADP]
[ATP] + [ADP] + [AMP]
0.002
0.852
0.037
0.224
0.124
0.869
0.956
0.417
300μg/mL Zym:
20μM GPi:
11mM Glucose:
100nM PMA:
10μM GPi:

Figure 5

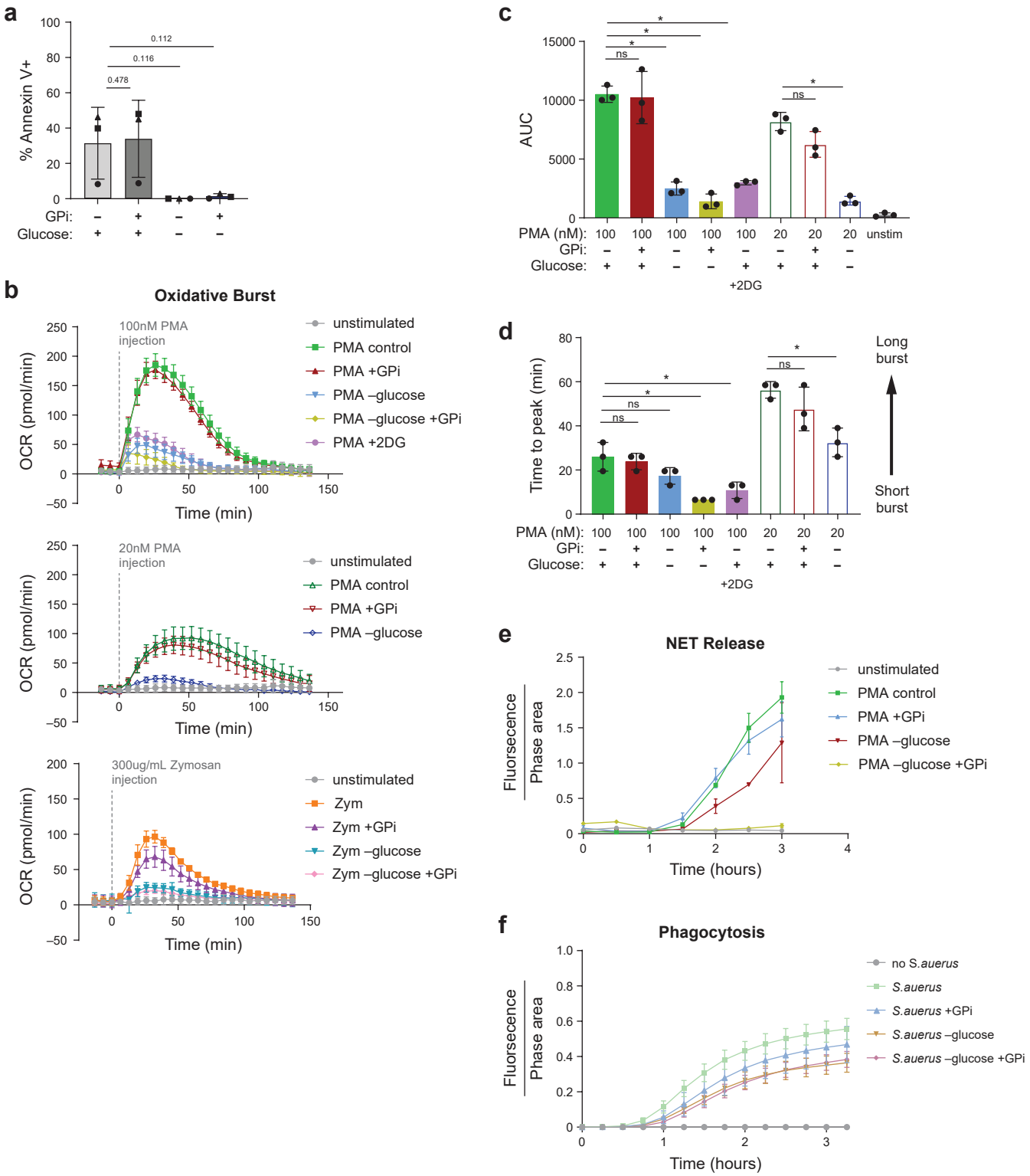
a
% Annexin V+
0.112
0.116
0.478
GPi:
Glucose:
b
Oxidative Burst
100nM PMA injection
OCR (pmol/min)
Time (min)
unstimulated
PMA control
PMA +GPi
PMA –glucose
PMA –glucose +GPi
PMA +2DG
20nM PMA injection
300ug/mL Zymosan injection
Zym
Zym +GPi
Zym –glucose
Zym –glucose +GPi
c
AUC
ns
PMA (nM):
unstim
+2DG
d
Time to peak (min)
Long burst
Short burst
e
NET Release
Fluorescence / Phase area
Time (hours)
f
Phagocytosis
no S.auerus
S.auerus
S.auerus +GPi
S.auerus –glucose
S.auerus –glucose +GPi

Figure 6

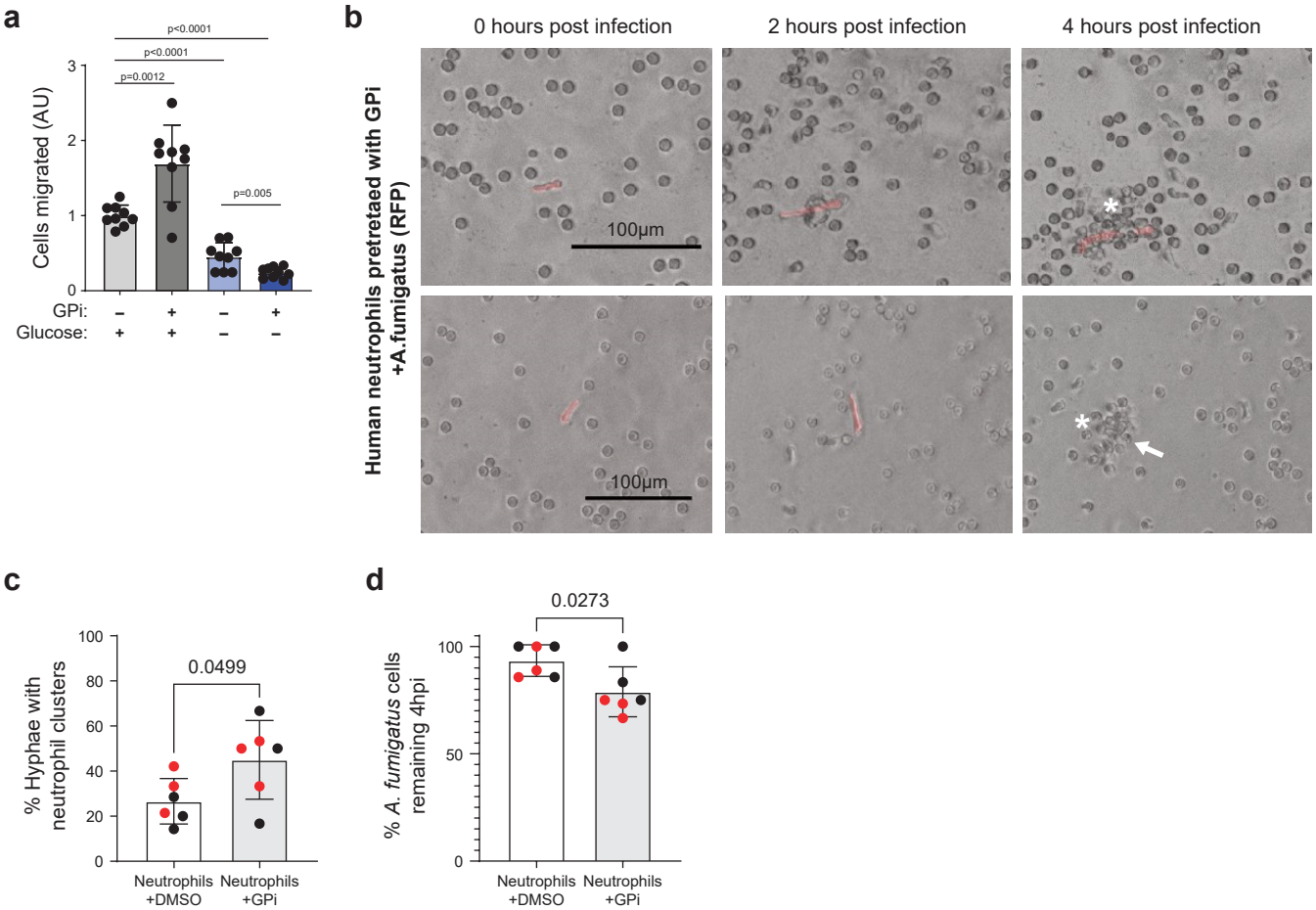
a
p<0.0001
p<0.0001
p=0.0012
p=0.005
Cells migrated (AU)
3
2
1
0
GPi: – + – +
Glucose: + + – –
b
0 hours post infection
2 hours post infection
4 hours post infection
Human neutrophils pretretaed with GPi +A.fumigatus (RFP)
100µm
100µm
c
0.0499
% Hyphae with neutrophil clusters
100
80
60
40
20
0
Neutrophils +DMSO
Neutrophils +GPi
d
0.0273
% A. fumigatus cells remaining 4hpi
100
50
0
Neutrophils +DMSO
Neutrophils +GPi

Supplemental Figure 1

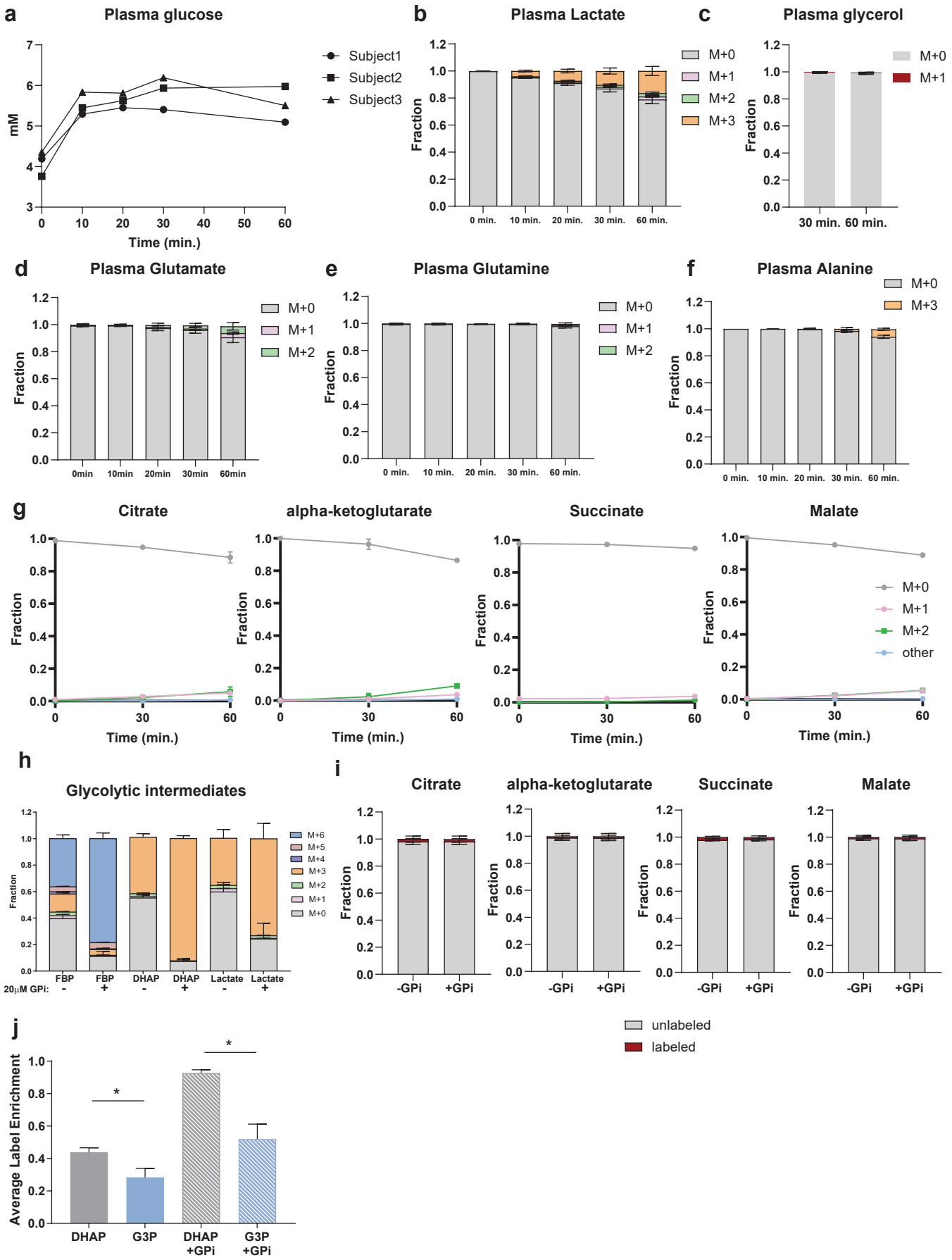

Supplemental Figure 2

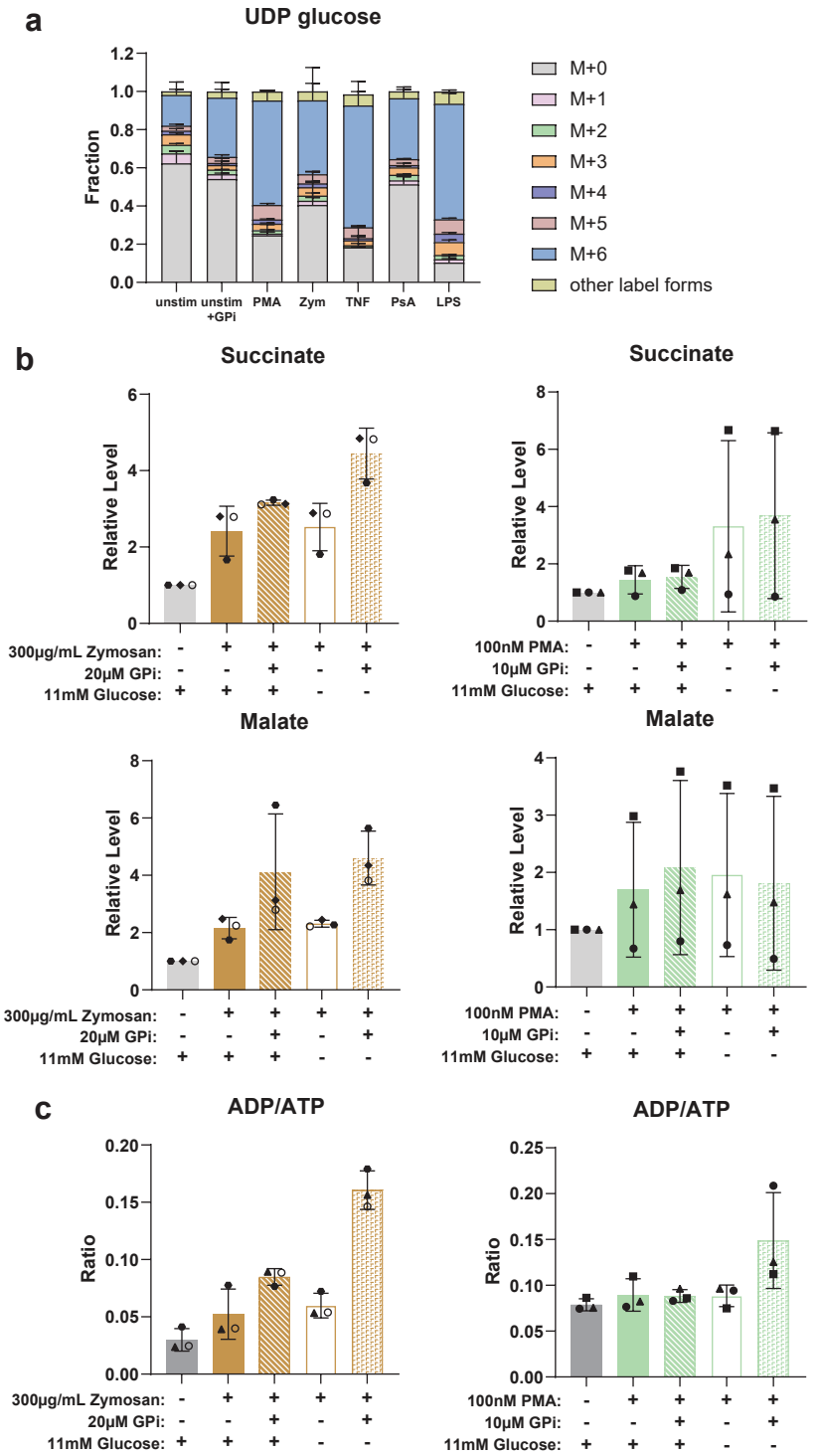

Supplemental Figure 3

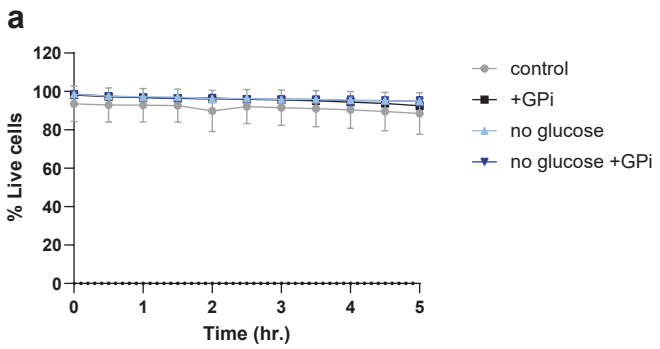

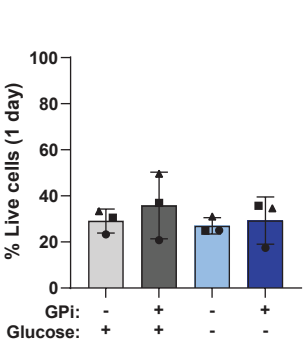
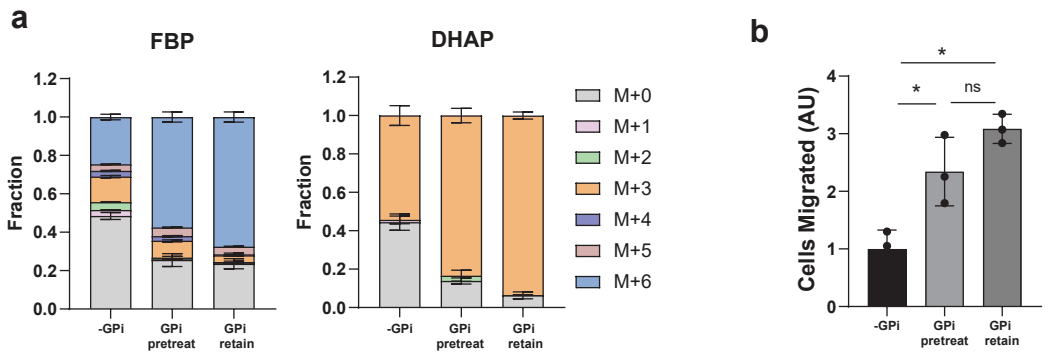
Supplemental Figure 4